INTERATOMIC POTENTIALS FOR MOLECULAR DYNAMICS SIMULATION

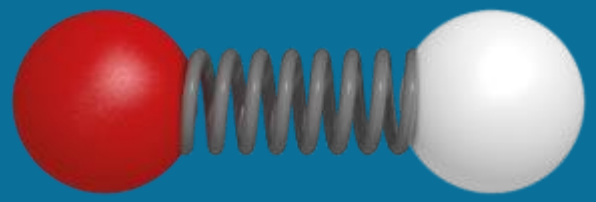

Alex Li

UC San Diego

Introduction – Molecular Dynamics and Potentials

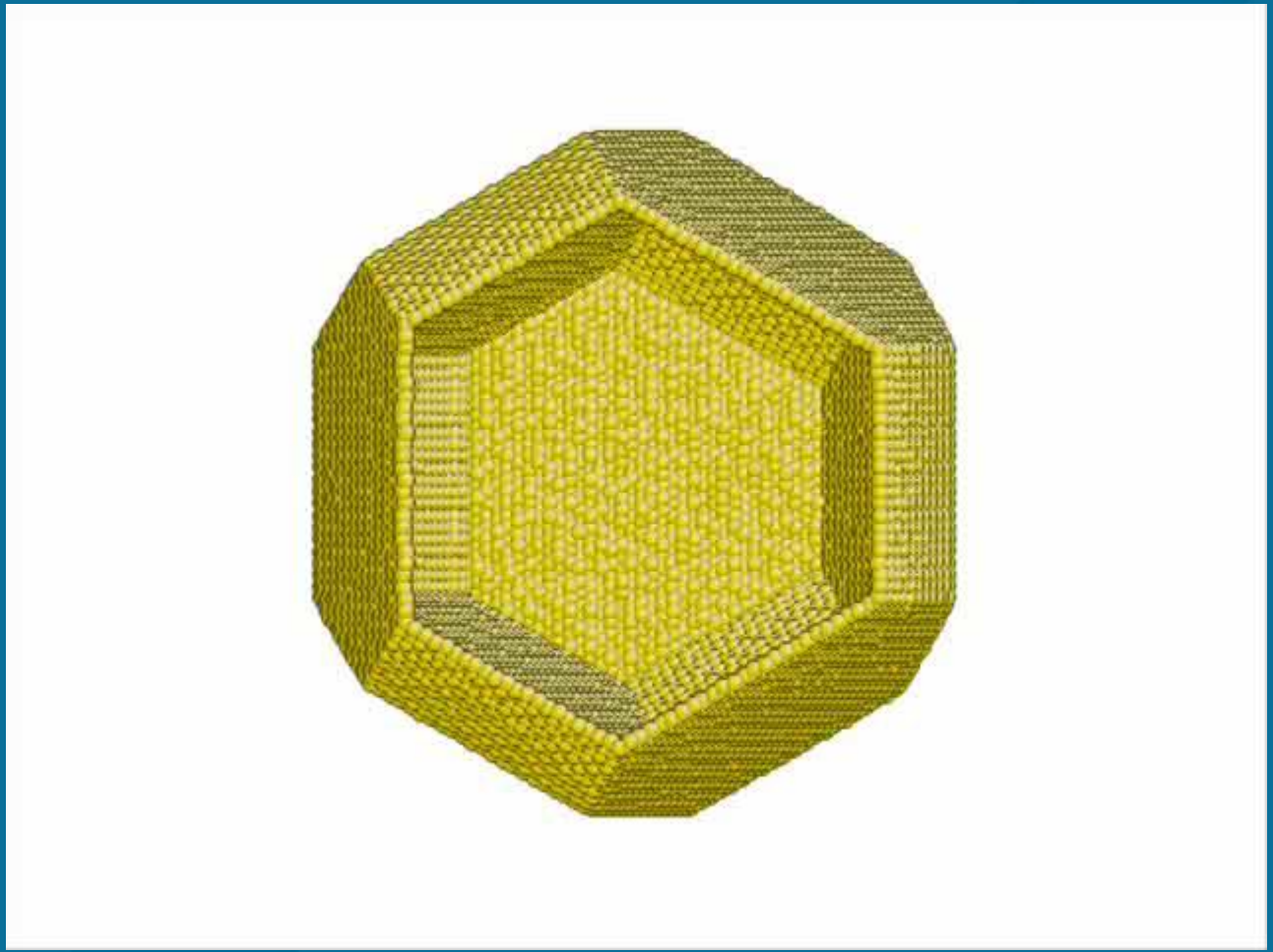

Dislocation Nucleation in Metallic Nanoparticles

- Molecular Dynamics
  - A simulation tool for analyzing the physical behavior of a system of particles
  - $F = ma$
    - Newton's laws applied to individual atoms
  - Interatomic Potentials
    - Describe the energy between particles, from which the forces can be derived
    - The accuracy of the potential translates to the accuracy of the simulation

Mordehai, Dan and Kazakevich, Michael and Srolovitz, David J. and Rabkin, Eugen, ACTA MATERIALIA, 2011

Types of Interatomic Potentials

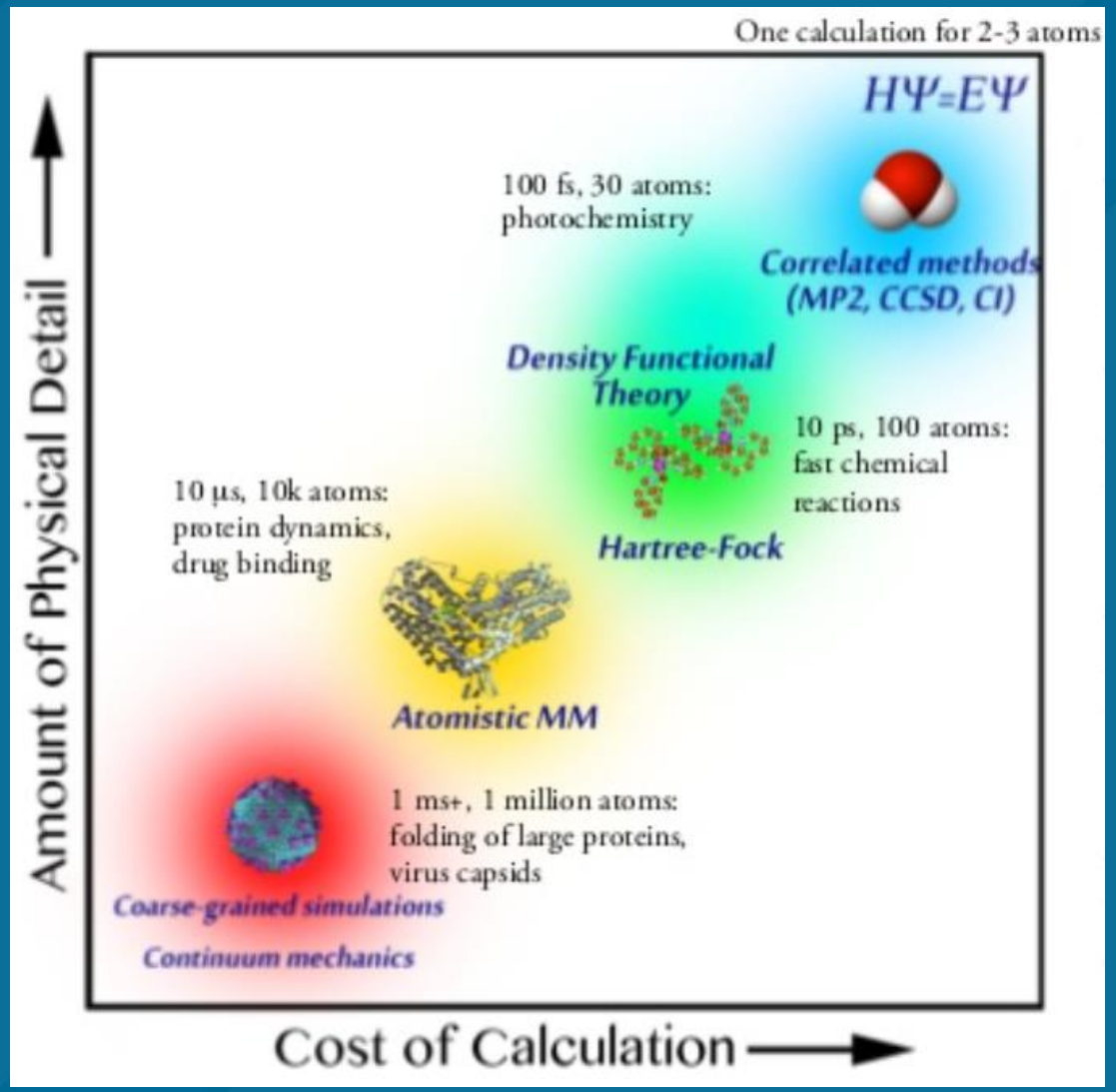

https://www.slideshare.net/bios203/bios203-lect4

- Interatomic Potentials describe the potential energy of a system of atoms
- There are many different Types of potentials with different resolution and computational load
  - Empirical Potentials
  - Ab Initio Methods
  - Machine Learning Potentials
- Multiscale Modeling
  - A method of bridging the scales from continuum mechanics to atomistic modeling

Lennard-Jones Potential

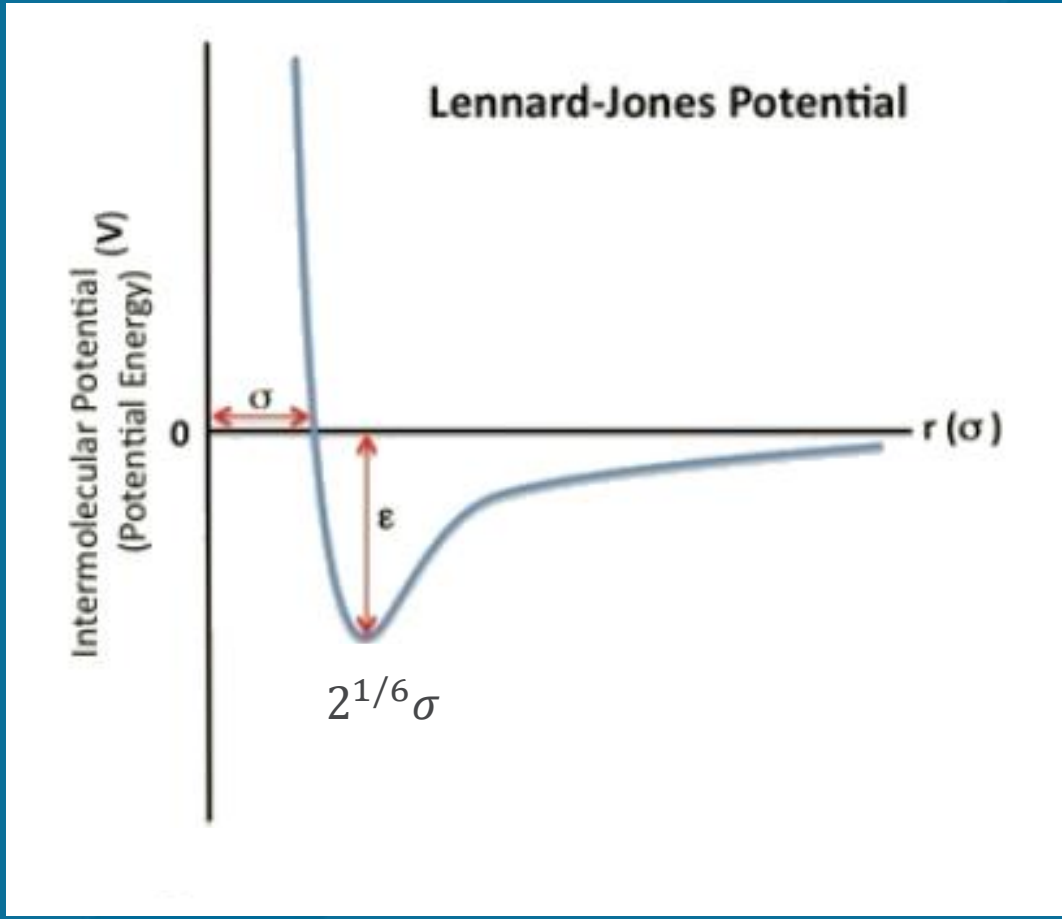

The deeper the well depth ε, the stronger the interaction between the two particles. When the bonding potential energy is equal to zero, the distance of separation, r, will be equal to σ. Minimum energy distance occurs at $2^{1/6}\,\sigma$.

$$V(r) = 4\varepsilon\left[\left(\frac{\sigma}{r}\right)^{12} - \left(\frac{\sigma}{r}\right)^{6}\right]$$

- Sometimes parameterized as
  - $V(r) = \frac{A}{r^{12}} - \frac{B}{r^{6}}$
    - Where $A = 4\varepsilon\sigma^{12}, B = 4\varepsilon\sigma^{6}$
- Widely known two-body potential
- Used as a basis for the two-body interaction in many higher order potentials

Lennard-Jones, *Royal Society*, 1924

Other Pair Potentials

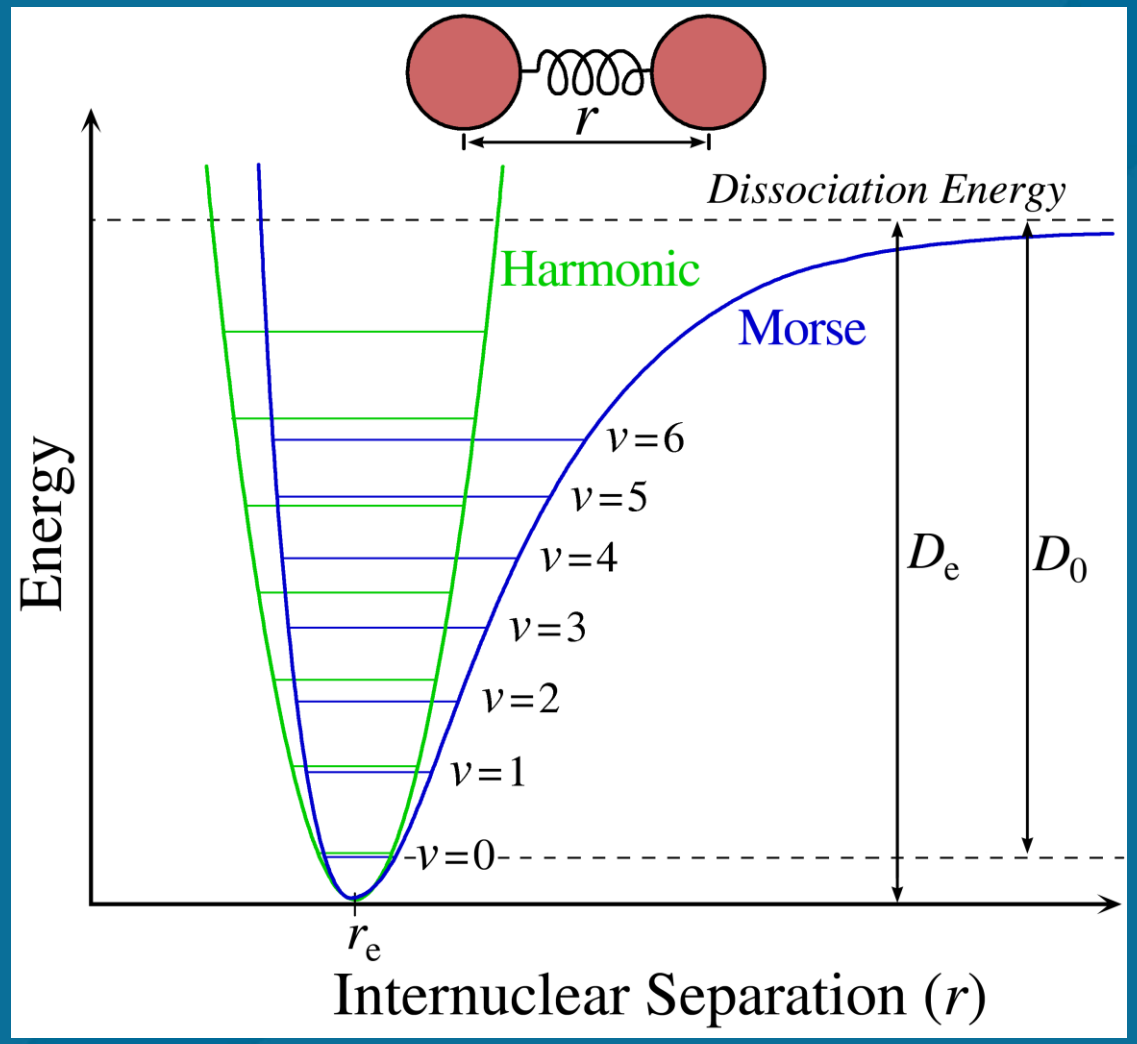

https://commons.wikimedia.org/wiki/File:Morse-potential.png

$$V(r) = D_e\left(e^{-2a(r-r_e)} - 2e^{-a(r-r_e)}\right)$$

- Morse Potential
  - Similarly composed of a repulsive and attractive term
- Buckingham Potential

$$\Phi_{12} = A\exp(Br)\frac{C}{r^6}$$

  - Considered a simplified LJ Potential

Morse, *Physical Review*, 1929 Buckingham, *Royal Society*, 1938

Lennard-Jones Potential - Applications

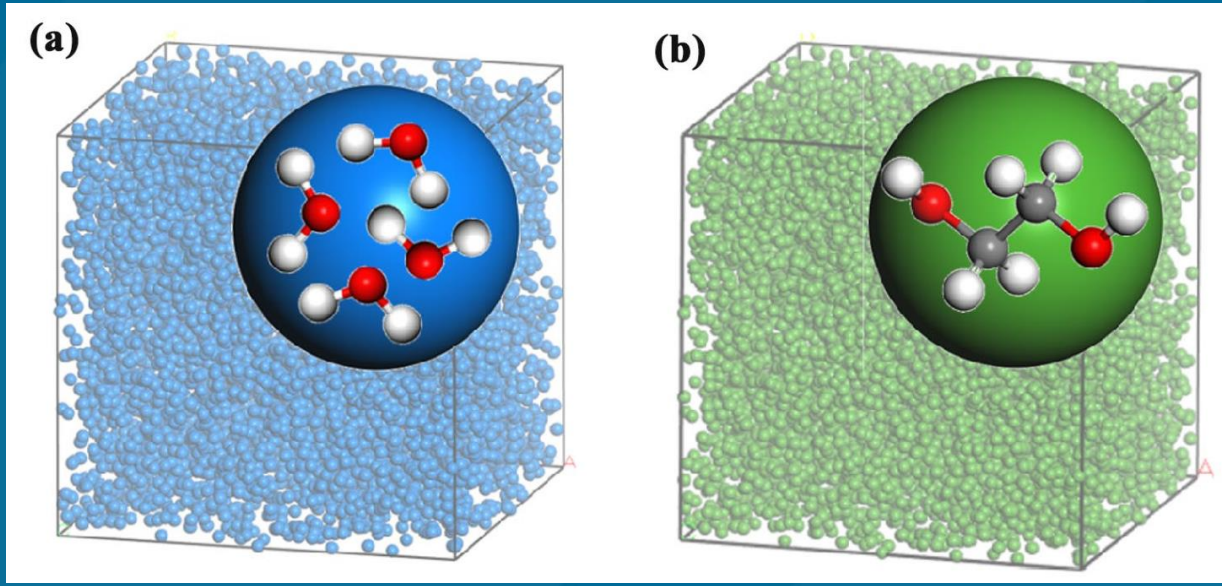

- Using the LJ to match physical properties of larger clusters of molecules for speeding up computation

Cha, J., Lee, W., Shin, E. *et al.* , *Multiscale Sci. Eng.*, 2020

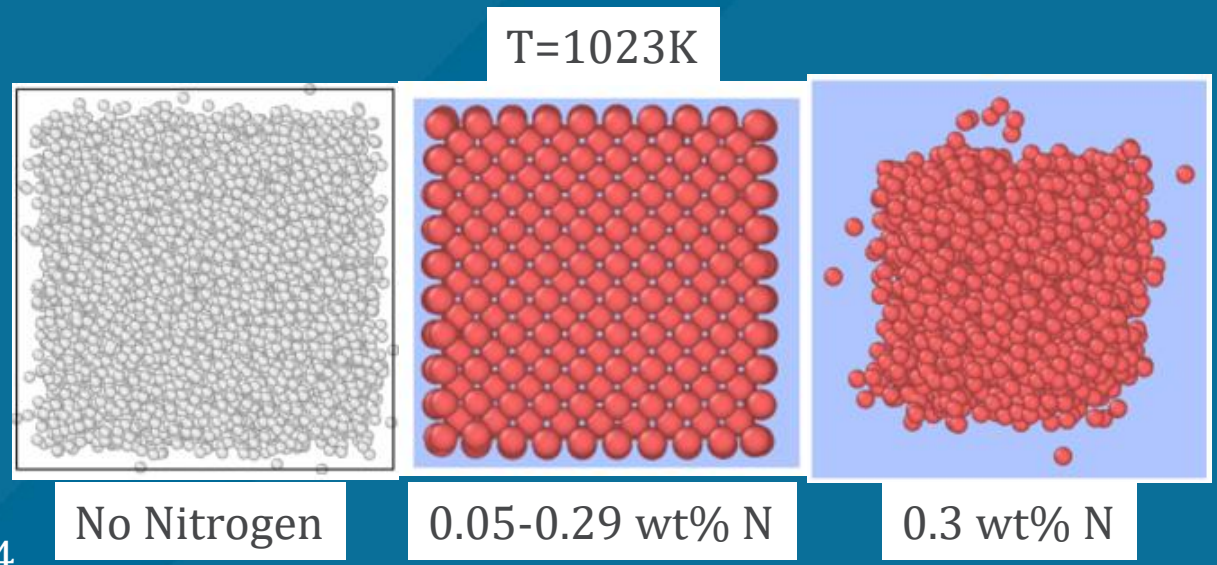

- Using LJ to derive properties of iron in molten lead for investigation of corrosion inhibition in nuclear reactors using Nitrogen

Triwardani et al. , *AIP Conference Proceedings*, 2020

Three Body Potentials

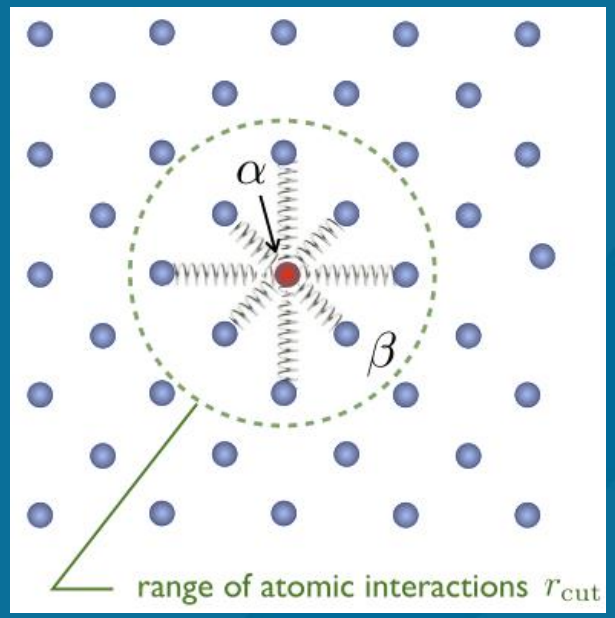

$$\mathcal{V} = \sum_{\alpha} \mathcal{V}^{\alpha} = \frac{1}{2} \sum_{\substack{\alpha,\beta \\ \alpha \neq \beta}} \phi(r^{\alpha\beta})$$

$$\mathcal{V} = \frac{1}{2!} \sum_{\substack{\alpha,\beta \\ \alpha \neq \beta}} \phi_2(r^{\alpha\beta}) + \frac{1}{3!} \sum_{\substack{\alpha,\beta,\gamma \\ \alpha \neq \beta \neq \gamma}} \phi_3(r^{\alpha\beta}, r^{\alpha\gamma}, r^{\beta\gamma})$$

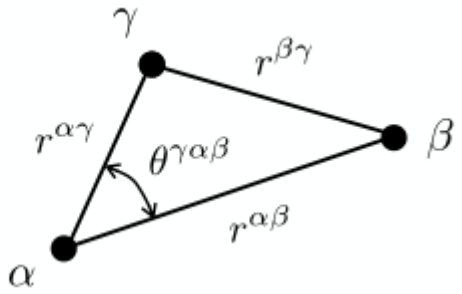

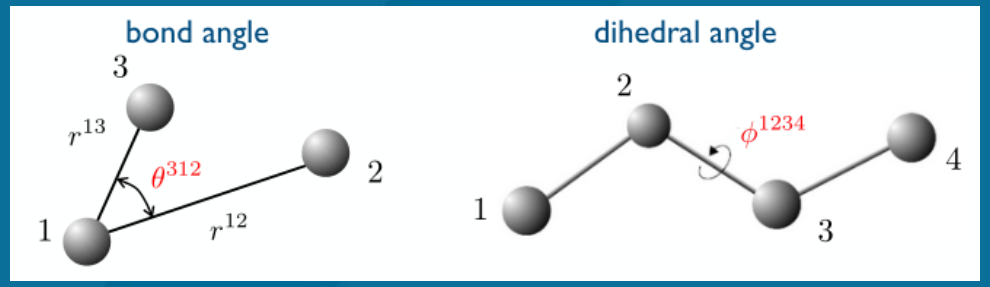

$$V = \frac{1}{2} \sum_{a,\beta \neq \alpha} \phi_2(r^{\alpha\beta}) + \frac{1}{6} \sum_{i,j} \phi_3(r^{\alpha\beta}, r^{\alpha\gamma}, \theta^{\gamma\alpha\beta})$$

Stilinger Weber

$$V = \frac{1}{2}\sum_{a,\beta\neq\alpha}\phi_2(r^{\alpha\beta}) + \frac{1}{3!}\sum_{i,j}\phi_3(r^{\alpha\beta}, r^{\alpha\gamma}, \theta^{\gamma\alpha\beta})$$

$$\phi_2(r) = f_c(r)\left[A_1 r^{-\lambda_1} - A_2 r^{-\lambda_2}\right]$$

$$f_c(r) = \begin{cases} e^{\mu/(r-r_{\text{cut}})} & \text{if } r < r_{\text{cut}} \\ 0 & \text{otherwise} \end{cases}$$

$$\phi_3(r^{\alpha\beta}, r^{\alpha\gamma}, \phi^{\beta\alpha\gamma}) = Z\left[f_c(r^{\alpha\beta})f_c(r^{\alpha\gamma})\right]\left(\cos\theta^{\beta\alpha\gamma} + \frac{1}{3}\right)^2$$

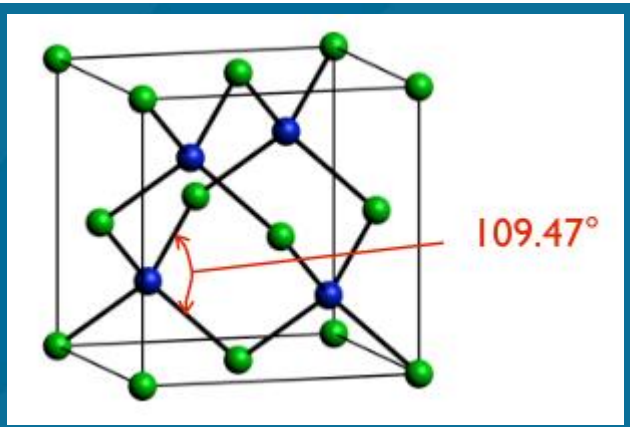

- Designed for Silicon
- Keating potential for pair-potential
- $\cos\theta^{\beta\alpha\gamma} + \frac{1}{3}$
  - This term is specific to the tetrahedral form of silicon, where $\theta_t = 109.47°$
    - $\cos\theta_t = -\frac{1}{3}$
    - This minimizes the energy in the tetrahedral configuration
- Parameters Used
  - $Z = 21, \mu = 1.20, r_{cut} = 1.80$
  - $A_1 = 7.049556277, A_2 = 0.6022246684$
  - $\lambda_1 = 4, \lambda_2 = 0$

Stillinger, F., Weber, T., *Physical Review B*, 1985

Stilinger Weber – Modeling Fracture in Graphene and CNT

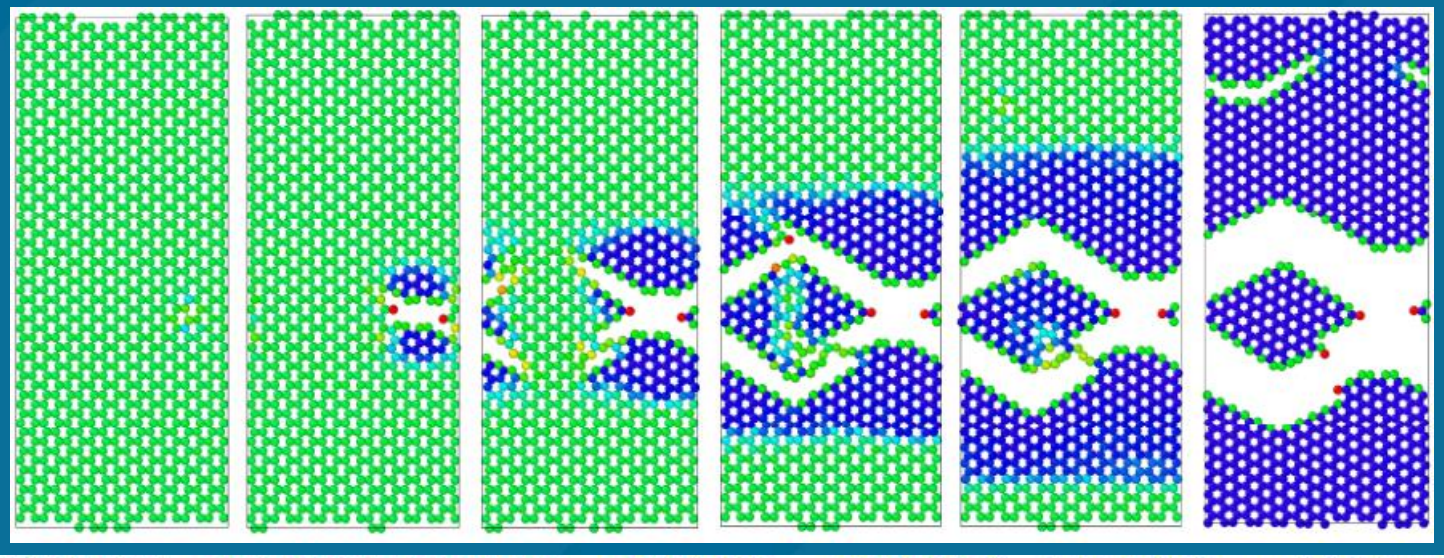

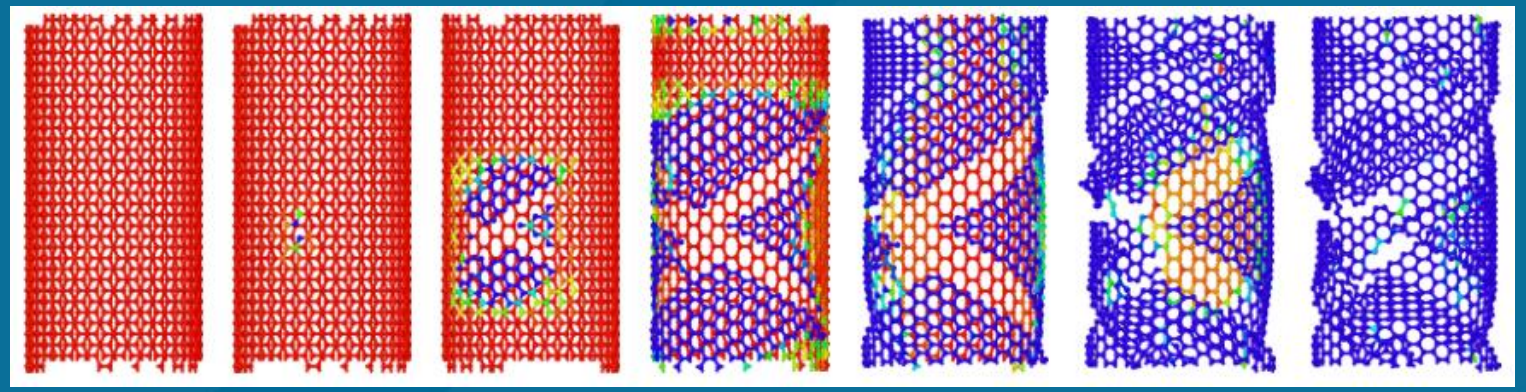

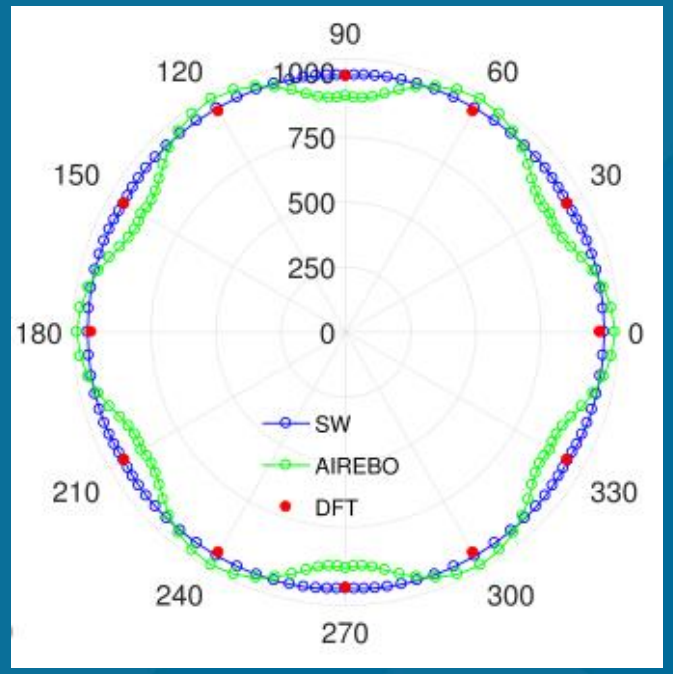

Young's Modulus vs Crystallographic Direction

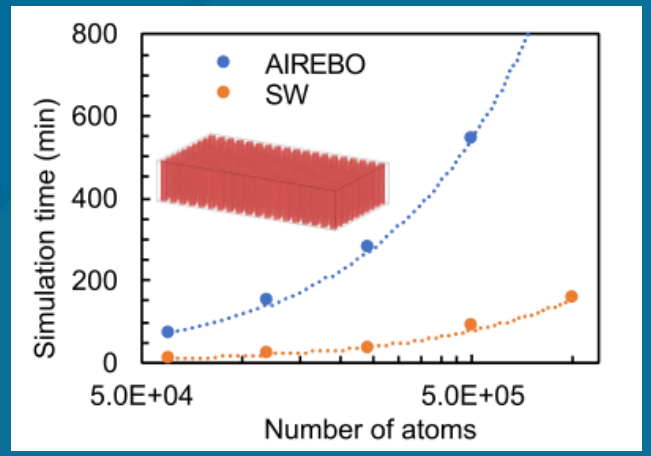

- Other empirical potentials did not exhibit glass-like brittle
- (ReaxFF, Tersoff, EDIP, AIREBO)

M Z Hossain et al, *J. Phys.: Condens. Matter,* 2018

Tersoff Potential

A Modified Two Body Potential

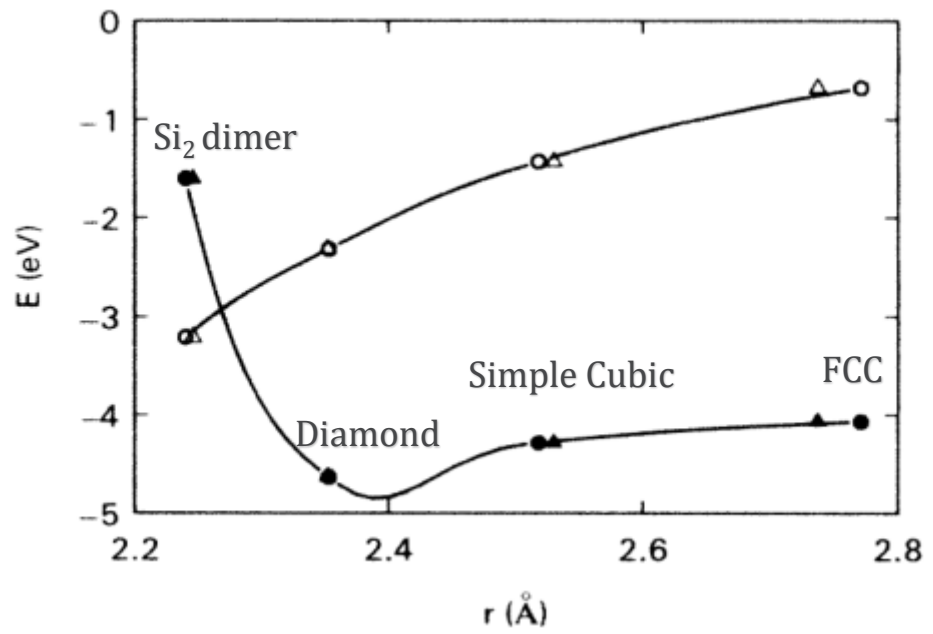

Silicon Energy vs Bond length
Open: Cohesive energy per bond
Closed: Cohesive energy per atom

$$E_{ij} = \sum_i E_i = \frac{1}{2}\sum_{i,j\neq i} V_{ij}$$

$$V_{ij} = f_c(r_{ij})\left[A\exp(-\lambda_1 r_{ij}) - B_{ij}\exp(\lambda_2 r_{ij})\right]$$

Tersoff Trial Potential

$$B_{ij} = B_0 \exp(-z_{ij}/b)$$

$$z_{ij} = \sum_{k\neq i,j} [w(r_{ik})/w(r_{ij})]^n \times \left[c + \exp(-d\cos\theta_{ijk})\right]^{-1}$$

$$w(r) = f_c(r)\exp(-\lambda_2 r)$$

$A = 2280$ eV, $B_0 = 171$ eV, $\lambda_1 = 2\lambda_2$, $\lambda_2 = 1.465$ Å^{-1}

$b = 1.324$, $c = 6.5$, $d = 6.02$, $n = 4$,

$$f_c = \begin{cases} 1, & r < R - D, \\ \frac{1}{2} - \frac{1}{2}\sin[\frac{1}{2}\pi(r-R)/D], & R - D < r < R + D, \\ 0, & r > R + D, \end{cases}$$

$R = 3.0$ Å, $D = 0.2$ Å

Tersoff, *Physical Review Letters*, 1985

Tersoff Potential – Modeling Mechanical Behavior in CMCs

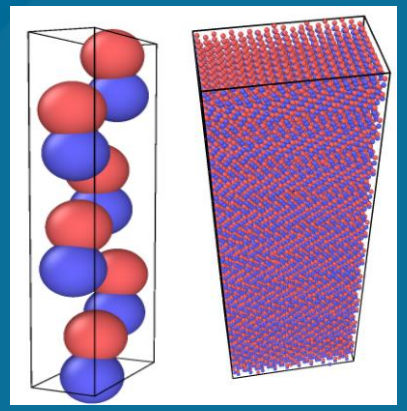

6H SiC

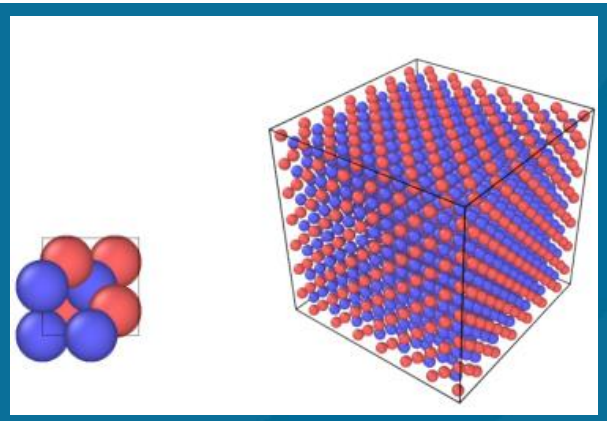

β-SiC (3H)

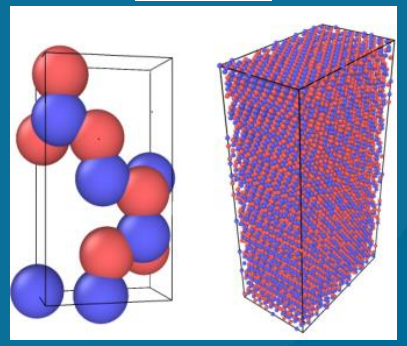

4H SiC

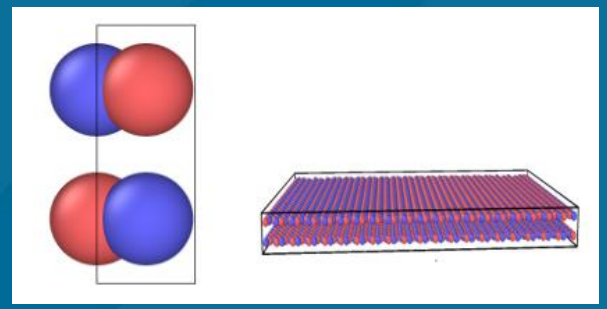

Bilayer h-BN

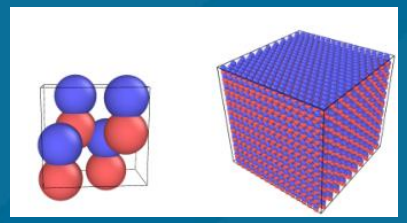

2H SiC

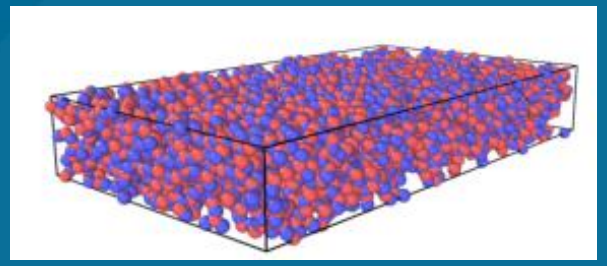

Amorphous BN

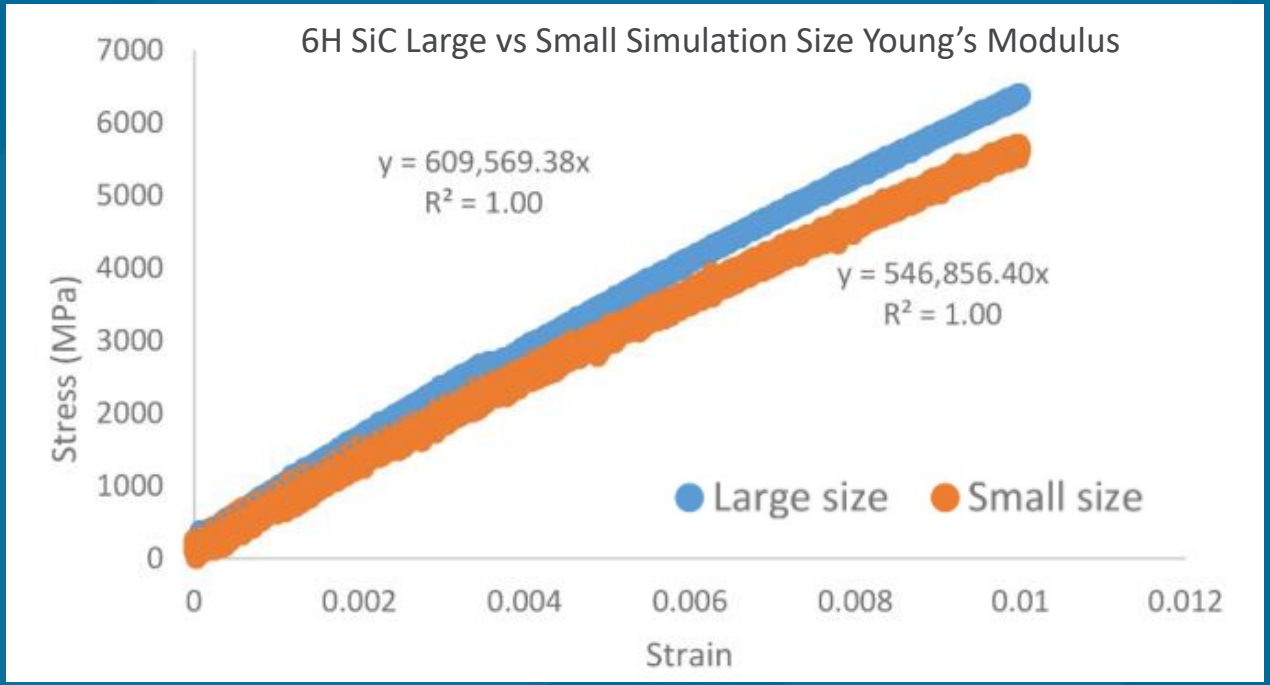

TABLE 1.—ELASTIC RESPONSE OF 6H SiC USING TERSOFF AT $\dot{\varepsilon} = 10^7/s$

Property	Sample 1	Sample 2	Sample 3	Average	Expt (Ref. 13)
E_x (GPa)	546.8560	537.768	544.946	543.19	473.417
E_y (GPa)	539.4410	536.8980	543.946	539.933	473.417
E_z (GPa)	612.0060	608.1430	633.749	617.966	544.188
G_{xy} (GPa)	252.7710	249.9730	254.459	252.401	195
G_{xz} (GPa)	225.9860	229.8690	221.512	225.789	163
G_{yz} (GPa)	219.4410	217.3560	219.582	218.793	163
ν_{xy}	0.23040	0.2188	0.2378	0.2290	0.2139
ν_{xz}	0.0840	0.0799	0.0797	0.0812	0.0739
ν_{yz}	0.0988	0.0941	0.0954	0.0961	0.0739

Aluko, O., Pineda, E., et al., *NASA-TM*, 2019

Embedded Atom Model

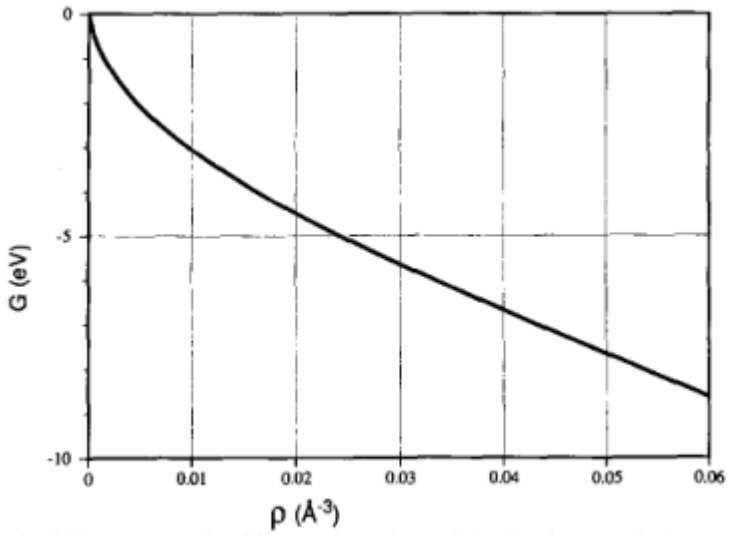

Embedding energy for Ni as a function of the background electron density.

$$E_{coh} = \sum_i G_i\left(\sum_{j\neq i} \rho_j^a(R_{ij})\right) + \frac{1}{2}\sum_{i,j\ (j\neq i)} U_{ij}(R_{ij})$$

G is embedding energy, ρ^a is the spherically averaged atomic electron density, and U is an electrostatic, two-atom interaction

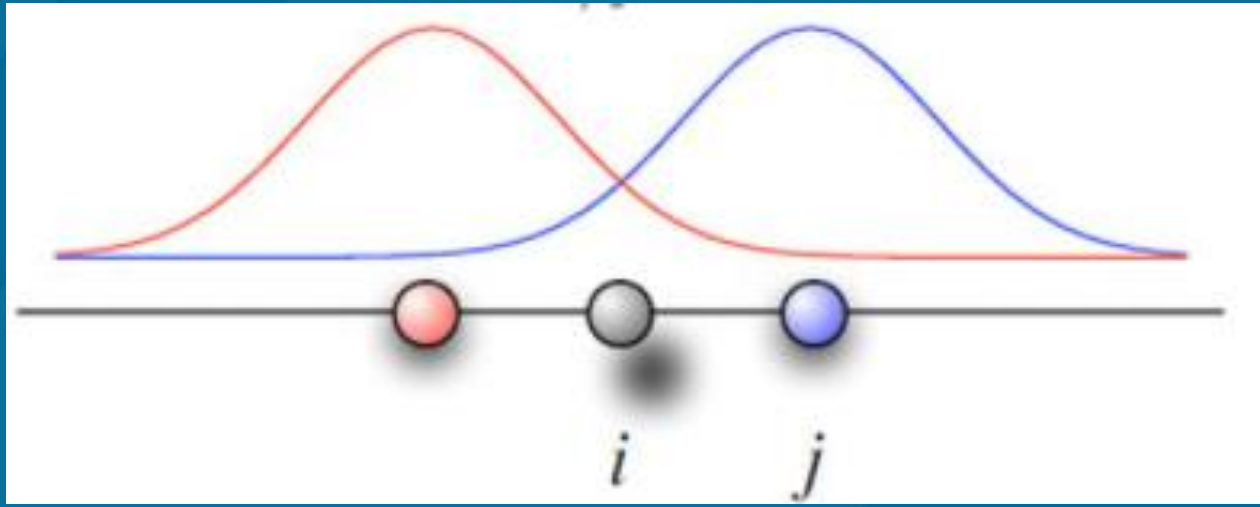

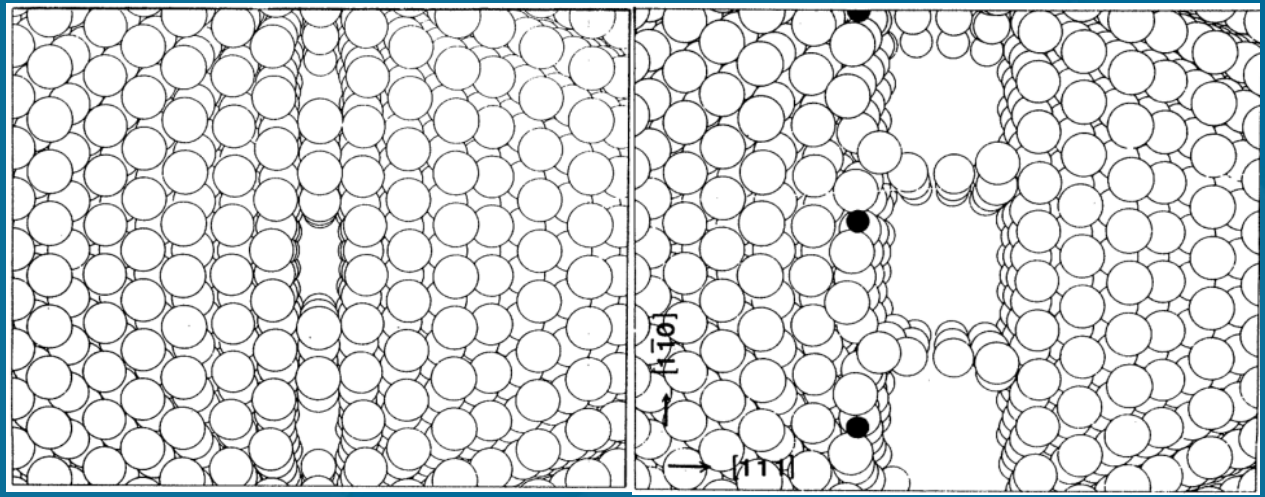

Ni Slab with defects. Hydrogen adsorption promotes fracture on the right side image

 Daw, M., Baskes, M., *Physical Review B*, 1983

Embedded Atom Model - Applications

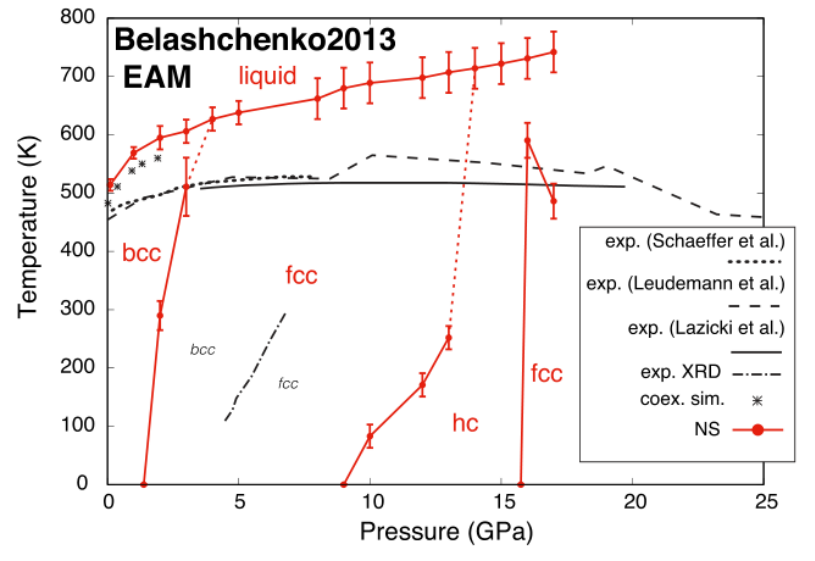

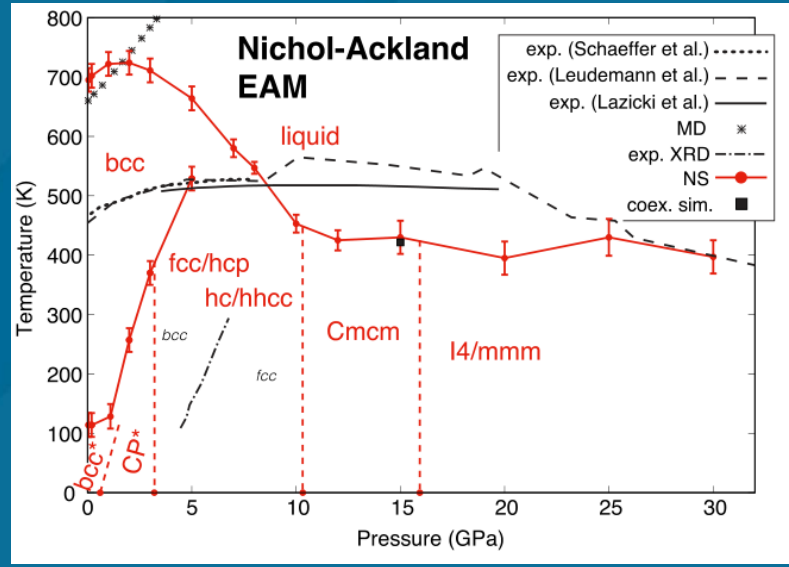

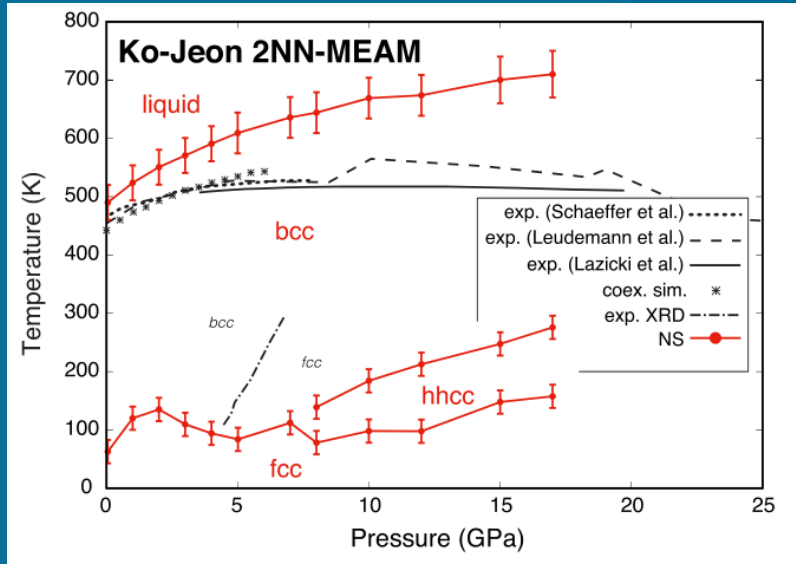

2NN-MEAM – Includes second nearest neighbor interactions

- Comparison of 3 phase diagrams constructed from different EAM models for Lithium
  - Fitted to different microstructural properties and using different procedures
  - Show differences in melting points, critical points, and phase transformations

 Jordan Dorrell and Livia B. Pártay, *The Journal of Physical Chemistry B*, **2020**

Wide Selection of Empirical Potentials

Silicon IMs since the 1980s:

1. Keating (Valence), *Phys. Rev.*, **145**, 637 (1966).
2. Altmann,...,Tomassini (Valence), *J. Phys. C*, **15**, 5581 (1982).
3. Pearson, Takai, Halicioglu, Tiller (PTHT), *J. Cryst. Growth*, **70**, 33 (1984).
4. Stillinger-Weber (SW), *PRB*, **31**, 5262 (1985).
5. Tersoff (T1), *PRL*, **56**, 632 (1986).
6. Brenner, Garrison, *PRB*, **34**, 1304 (1986).
7. Dodson (DOD), *PRB*, **35**, 2795 (1987).
8. Biswas, Hamann (BH), *PRB*, **36**, 6434 (1987).
9. Baskes (EAM-Si), *PRL*, 2666 (1987).
10. Tersoff (T2), *PRB*, **37**, 6991 (1988).
11. Tersoff (T3), *PRB*, **38**, 9902 (1988).
12. Khor, Das Sarma, *PRB*, **38**, 3318 (1988).
13. Kaxiras, Pandey, *PRB*, **38**, 12736 (1988).
14. Baskes, Nelson, Wright (MEAM-Si), *PRB*, **40**, 6085 (1989).
15. Ackland, *PRB*, **40**, 10351 (1989).
16. Chelokowsky, Phillips, Kamal, Strauss, *PRL*, **62**, 292 (1989).
17. Mistriotis, Flytzanis, Farantos (4-body), *PRB*, **39**, 1212 (1989).
18. Erkoç, *Phys. Stat. Sol. (b)*, **152**, 447 (1989).
19. Bolding, Anderson, *PRB*, **41**, 10568 (1990).
20. Carlsson, Fedders, Myles, *PRB*, **41**, 1247 (1990).
21. Murrell, Mottram, *Mol. Phys.*, **69**, 571 (1990).
22. Wang, Rockett, *PRB*, **43**, 12571 (1991).
23. Chelikowsky, Glassford, Phillips, *PRB*, **44**, 1538 (1991).
24. Li, Johnson, Murrell, *Chem. Soc. Faraday Trans.*, **88**, 1229 (1992).
25. Gong, *PRB*, **47**, 2329 (1993).
26. Liu, *Thermocem. J. Molec. Struct.*, **341**, 253 (1995).
27. Omote, Waseda (Pair Potential), *Jap. J. Appl. Phys. 1*, **35**, 151 (1996).
28. Stephenson, Radny, Smith (modifed SW), *Surf. Sci.*, **366**, 177 (1996).
29. Bazant, Kaxiras, Justo (EDIP), *PRB*, **56**, 8542 (1997).
30. Cai, *Phys. Stat. Sol. B*, **212**, 9 (1999).
31. Lenosky,...,Kress (MEAM), *Mod. Sim. Mater. Sci. Eng.*, **8**, *825 (2000)*.
32. van Duin,...,Goddard (ReaxFF), *J. Phys. Chem. A* **107**, 3803 (2003).
33. Erhart, Albe (Bond Order), *PRB*, **71**, 035211 (2005).
34. Kumagai, Izumi, Hara, Sakai, *Comp. Mat. Sci*, **39**, 457 (2007).
35. Lee, *Calphad-Comp. Coupling Phase Diag. Thermochem.*, **31**, 95 (2007).
36. Yu, Sinnott, Phillpot, *PRB*, **75**, 085311 (2007).
37. Timonova, Lee, Thijsse (MEAM), *Nuc. Inst. Meth. Phys. Res. B*, **255**, 195 (2007).
38. Gillespie,...,Pettifor (Bond Order), *PRB*, **75**, 155207 (2007).
39. Behler and Parrinello (NN), *Phys. Rev. Lett.* **98**, 146401 (2007).
40. Vashishta et al. (3-body), *J. Appl. Phys.* **101**, 103515 (2007).
41. Sanville (NN), *J. Phys. Cond. Matt.* **20**, 285219 (2008).
42. Schelling (Bond order), *Comp. Mat. Sci.* **44**, 274-279 (2008)
43. Malshe et al. (NN), *J. Chem. Phys.* **129**, 044111 (2008).
44. Ohta et al. (SW), *Jap. J. Appl. Phys.* **48**, 020225 (2009).
45. Hossain et al. (DFT-ArSi), *Nucl. Inst. & Meth. Phys. Res. B* **267**, 1061 (2009).
46. Lucas et al. (EDIP), *J. Phys. Cond. Matt.* **22**, 035802 (2010).
47. Ryu and Cai (MEAM), *J. Phys. Cond. Matt.* **22**, 055401 (2010).
48. Timonova and Thijsse (MEAM), *Comp. Mat.. Sci.* **48**, 609-620 (2010).
49. Grochia et al. (MEAM), *Chem. Phys. Lett.* **493**, 57-60 (2010).
50. Du et al. (MEAM), *Phys. Stat. Solidi B* **248**, 2050-2055 (2011).
51. Tewary (Phenomenological), *Phys. Lett. A* **375**, 3811-3816 (2011).
52. Lee and Hwang (FM-SW), *Phys. Rev. B* **85**, 125204 (2012).
53. Dongare et al. (A-EAM), *MSMSE* **20**, 035007 (2012).
54. Cui et al. (MEAM), *J. Power Sources* **207**, 150-159 (2012).
55. da Cruz et al. (MEAM), *J. Heat Trans.* **134**, 062402 (2012).
56. Briquet et al., (reactive) *J. Phys.: Condens. Matter.* **24**, 395004 (2012).
57. Pastewka et al. (Bond Order). *PRB* **87**, 205410 (2013).
58. Saidi et al. (MEAM). *MSMSE* **22**, 055010 (2014).
59. Jaramillo-Botero et al. (ReaxFF). *J. Chem. Theory Compt.* **10**, 1426 (2014).
60. Takamoto et al. (Tersoff). *J. Appl. Phys.* **120**, 165109 (2016).
61. Pun and Mishin (Tersoff). *PRB* **95**, 224103 (2017).
62. Bartok et al. (machine learning), *PRX* **8**, 041048 (2018).

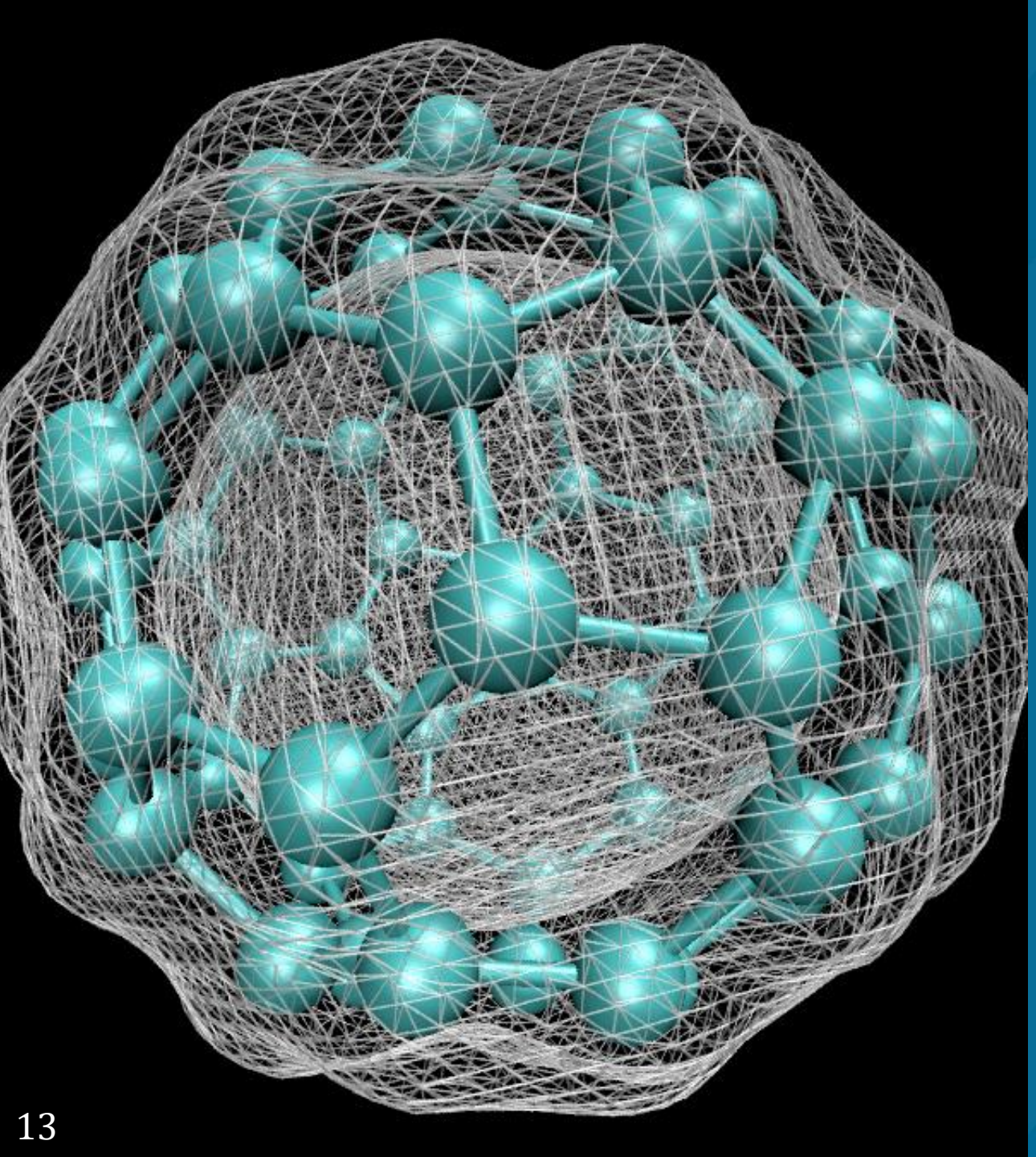

Density Functional Theory

https://en.wikipedia.org/wiki/Density_functional_theory#/media/File:C60_isosurface.png

Density Functional Theory

Walter Kohn

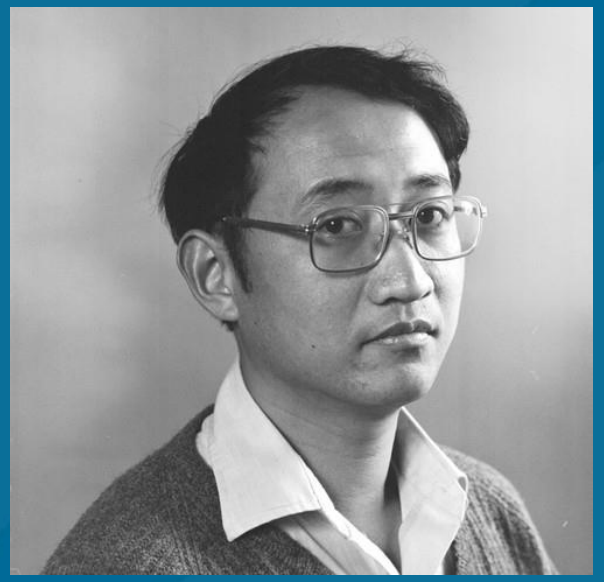

Lu Jeu Sham

$$-\frac{1}{2}\nabla^2\phi_i(\vec{r}) + \left[V_{ext}(\vec{r}) + \underbrace{\int d\vec{r}\,'\frac{n(\vec{r}\,')}{|\vec{r}-\vec{r}\,'|}}_{V_H} + \underbrace{\epsilon_{xc}[n] + n(\vec{r})\frac{\delta\epsilon_{xc}[n]}{\delta n(\vec{r})}}_{V_{xc}}\right]\phi_i(\vec{r}) = \varepsilon_i\phi_i(\vec{r})$$

Kohn – Sham Equation

- The Schrodinger Equation:

$$\hat{\mathrm{H}}|\Psi\rangle = E|\Psi\rangle$$

- Governs dynamics of a time-independent system
- Ψ is the many electron wave function
  - Contains 3N degrees of freedom, where N is the number of electrons
- Density Functional Theory reduces the complexity of the system from a 3N Body problem to N single body problems
  - Theorem 1 - The external potential is a unique functional of the electron density only. Thus the Hamiltonian, and hence all ground state properties, are determined solely by the electron density.
  - Theorem 2 - The groundstate energy may be obtained variationally: the density that minimizes the total energy is the exact groundstate density.

 Kohn, W., Sham, L., *Physical Review*, 1965

Density Functional Theory

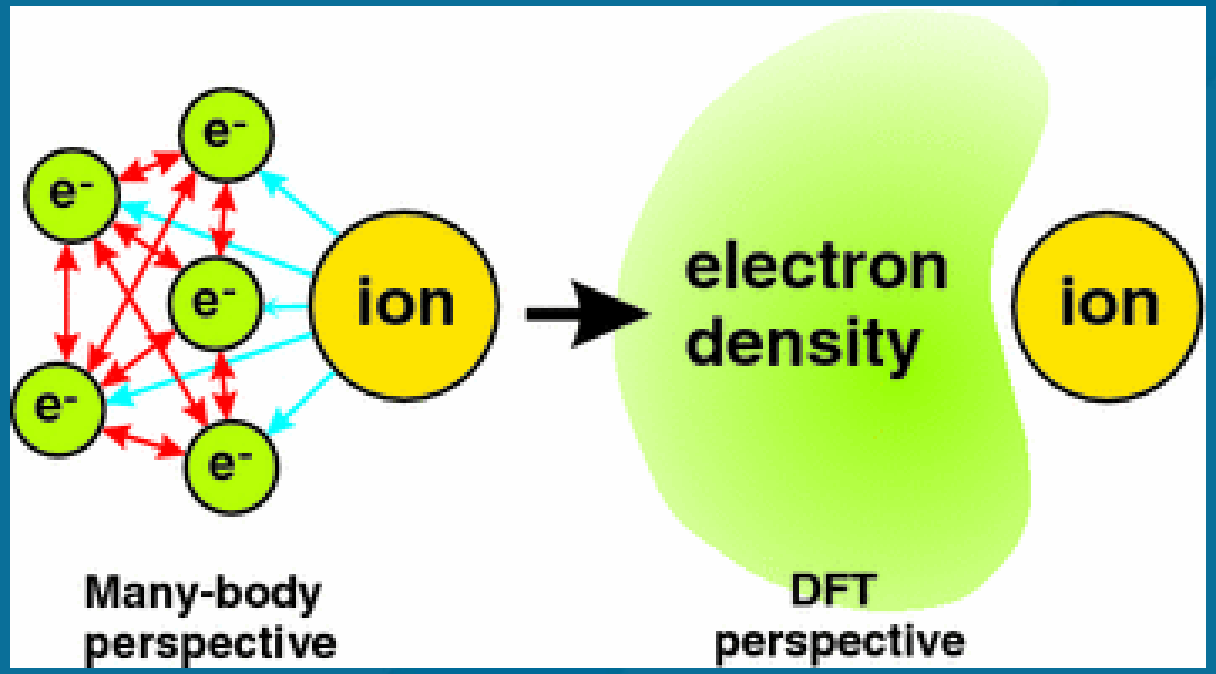

Bechstedt F. (2015) Density Functional Theory

$$-\frac{1}{2}\nabla^2\phi_i(\vec{r}) + \left[V_{ext}(\vec{r}) + \underbrace{\int d\vec{r}\,'\frac{n(\vec{r}\,')}{|\vec{r}-\vec{r}\,'|}}_{V_H} + \underbrace{\epsilon_{xc}[n] + n(\vec{r})\frac{\delta\epsilon_{xc}[n]}{\delta n(\vec{r})}}_{V_{xc}}\right]\phi_i(\vec{r}) = \varepsilon_i\phi_i(\vec{r})$$

Kohn – Sham Equation

- The Schrodinger Equation:

$$\hat{\mathrm{H}}|\Psi\rangle = E|\Psi\rangle$$

- Governs dynamics of a time-independent system
- Ψ is the many electron wave function
  - Contains 3N degrees of freedom, where N is the number of electrons
- Density Functional Theory reduces the complexity of the system from a 3N Body problem to N single body problems
  - Theorem 1 - The external potential is a unique functional of the electron density only. Thus the Hamiltonian, and hence all ground state properties, are determined solely by the electron density.
  - Theorem 2 - The groundstate energy may be obtained variationally: the density that minimizes the total energy is the exact groundstate density.

 Kohn, W., Sham, L., *Physical Review*, 1965

Density Functional Theory in MD – Car-Parrinello

$$\mathcal{L}_{\mathrm{CP}} = \frac{1}{2}\sum_I M_I \dot{\mathbf{R}}_I^2 + \frac{\mu}{2}\sum_i \langle \dot{\Phi}_i \mid \dot{\Phi}_i \rangle$$
$$- E(\mathbf{R}, \{\Phi\}) + \sum_{ij} \lambda_{ij} \left(\langle \Phi_i \mid \Phi_j \rangle - \delta_{ij} \right),$$

Lagrangian (Kinetic minus Potential Energy)

$$M_I \ddot{\mathbf{R}}_I = -\frac{\partial E(\mathbf{R}, \{\Phi\})}{\partial \mathbf{R}_I} + \sum_{ij} \lambda_{ij} \frac{\partial}{\partial \mathbf{R}_I} \langle \Phi_i \mid \Phi_j \rangle,$$
$$\mu \ddot{\Phi}_i = -\mathcal{H}(\mathbf{R}, \{\Phi\})\Phi_i + \sum_j \lambda_{ij} \Phi_j,$$

Equations of Motion

$$E_{\mathrm{const}} = \frac{1}{2}\sum_I M_I \dot{\mathbf{R}}_I^2 + \frac{\mu}{2}\sum_i \langle \dot{\Phi}_i \mid \dot{\Phi}_i \rangle + E(\mathbf{R}, \{\Phi\}),$$
$$= E_{\mathrm{phys}} + \frac{\mu}{2}\sum_i \langle \dot{\Phi}_i \mid \dot{\Phi}_i \rangle = E_{\mathrm{phys}} + T_{\mathrm{e}}.$$

Constant of Motion

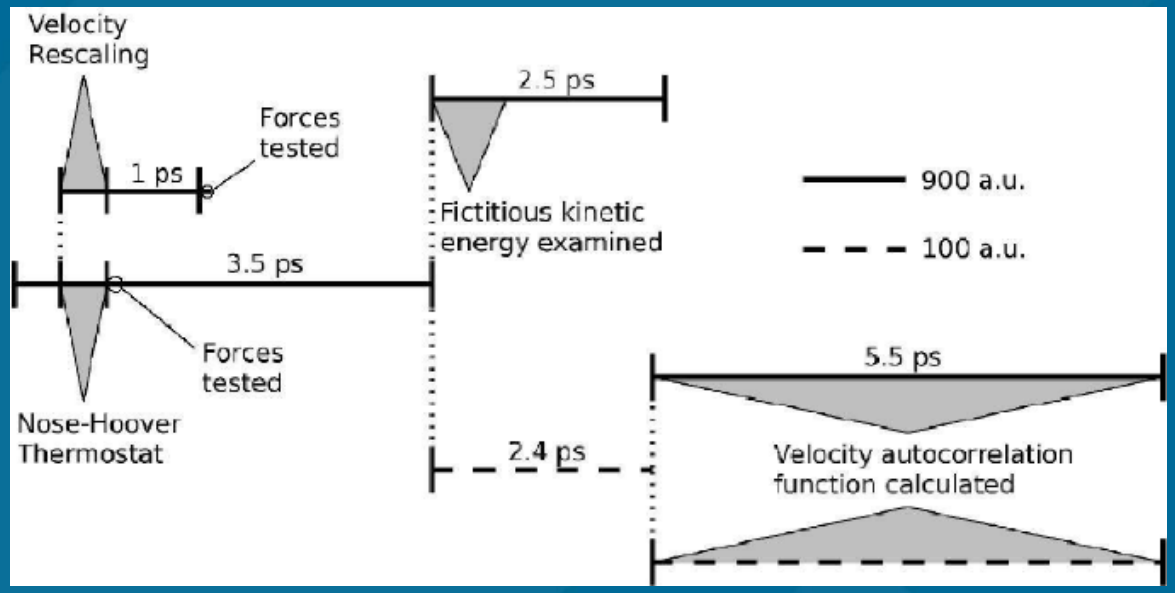

- Lagrangian form assigns Newtonian dynamics to both the ionic nuclei and the electron orbitals themselves
- A fictitious mass parameter is assigned to the electron orbitals
  - Large enough to allow large timesteps
  - Small enough not to affect nuclei

Car, R., Parinello, M., *Physical Review Letters*, 1985

Density Functional Theory in MD – Born-Oppenheimer

$$\mathcal{L}(\mathbf{q}, \dot{\mathbf{q}}, \mathbf{x}, \dot{\mathbf{x}}) = \frac{1}{2}M\dot{\mathbf{q}}^2 + \frac{1}{2}\mu\dot{\mathbf{x}}^2 - E(\mathbf{q}, \mathbf{y}) + k\mu G(\|\mathbf{x} - \mathbf{y}\|),$$

$$\mathcal{L}_{\mathrm{BO}}(\mathbf{R}, \dot{\mathbf{R}}) = \frac{1}{2}M\dot{\mathbf{R}}^2 - E(\mathbf{R}),$$

$$E(\mathbf{R}) = \min_{\{\Phi\}}\left[E_{\mathrm{KS}}(\mathbf{R}, \{\Phi\}) - \sum_{ij}\lambda_{ij}\left(\langle\Phi_i|\Phi_j\rangle - \delta_{ij}\right)\right],$$

$$\mathcal{L}_{\psi}(\psi, \dot{\psi}) = \frac{1}{2}\sum_i \dot{\psi}_i^2 + kG(\{\psi\}, \{\Phi\}).$$

- Born-Oppenheimer Molecular Dynamics are very similar to Car-Parinello
  - Lagrangian representation of system energy dynamics
  - Electronic waveform remains on the Born-Oppenheimer potential energy surface
- Born Oppenheimer calculates the electronic wave function differently
  - Car-Parinello uses fictitious dynamics to propagate
  - Born-Oppenheimer solves the wave function at each time step
- Born Oppenheimer has larger timesteps but more costly computation
  - Higher accuracy
- More used as computational power has increased

 WIREs, Comput Mol Sci, 2012

Ab initio Molecular Dynamics in action

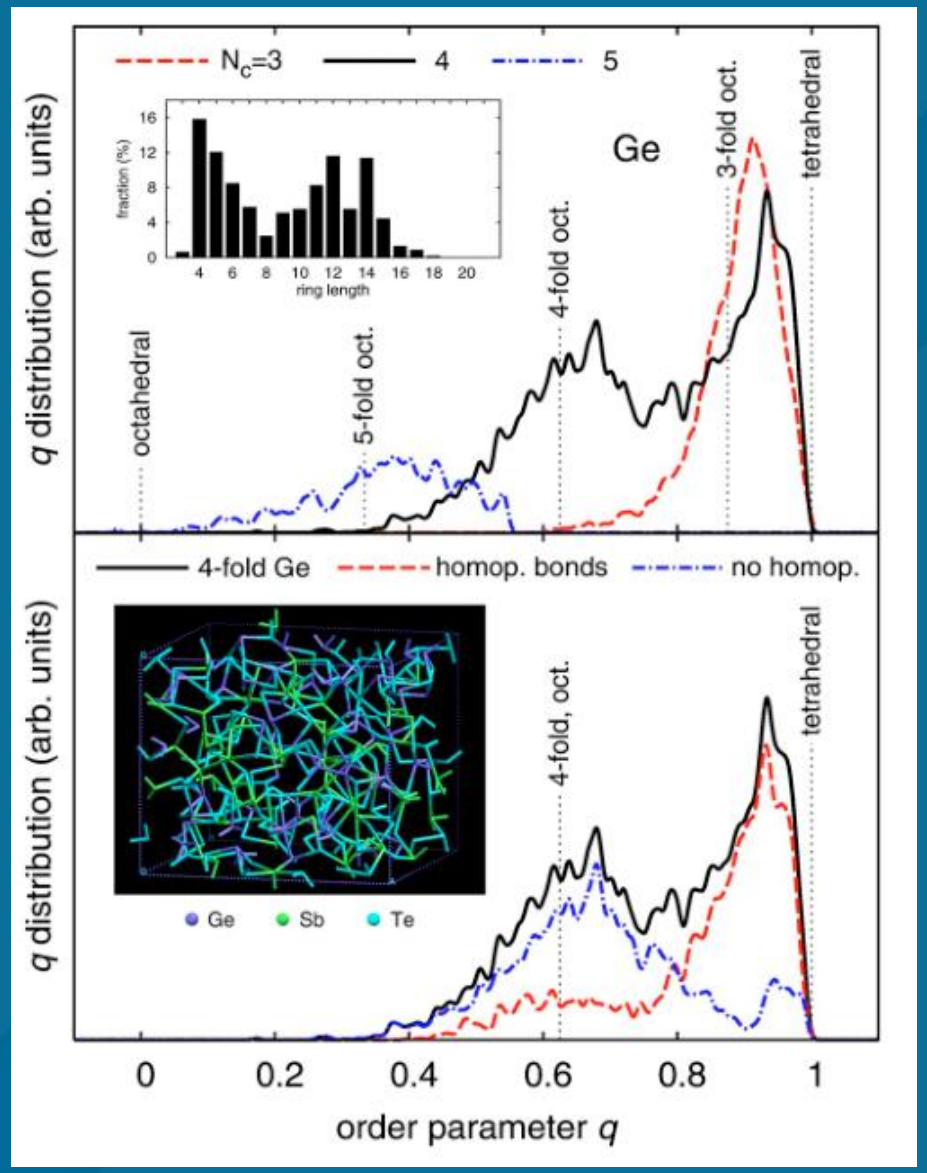

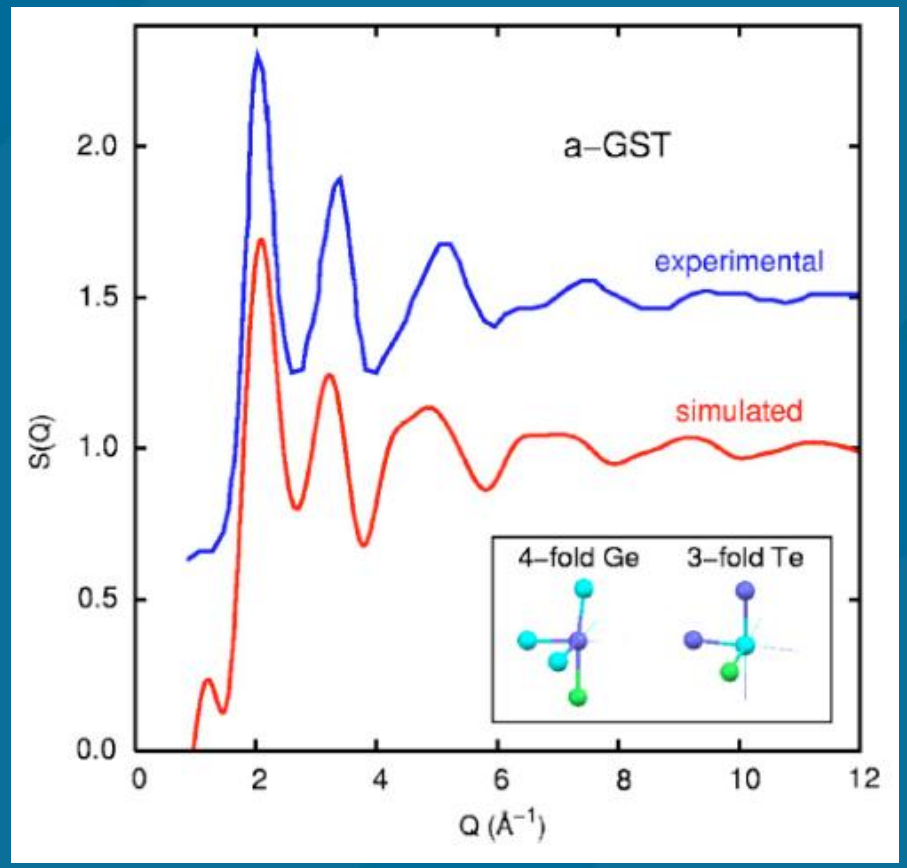

- Experimental and simulated XRD for amorphous GST
- Order Parameters for different coordinations

 S. Caravati et al., *Appl. Phys. Lett.* 2007

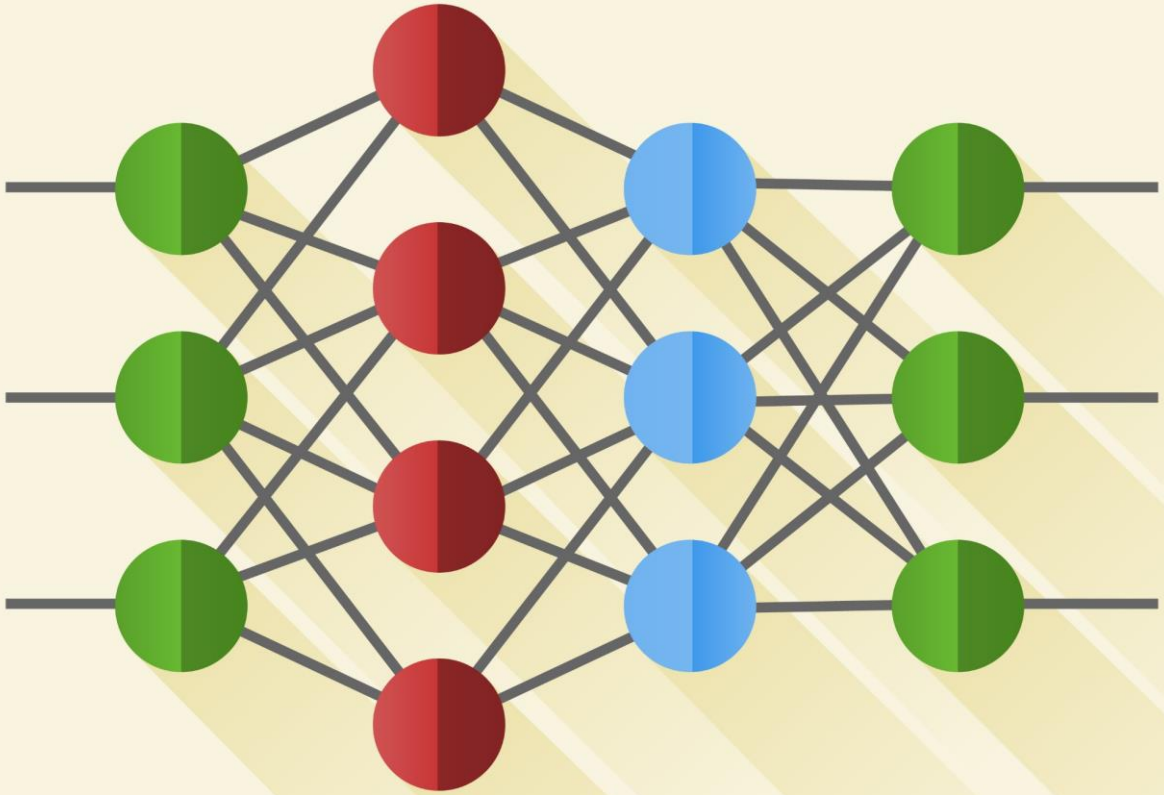

https://brighterion.com/artificial-intelligence-101-neural-networks/

Machine Learning and Interatomic Potential Development

The underlying physical laws necessary for the mathematical theory of a large part of physics and the whole of chemistry are thus completely known, and the difficulty is only that the exact application of these laws leads to equations much too complicated to be soluble. It therefore becomes desirable that approximate practical methods of applying quantum mechanics should be developed.

~Paul A.M. Dirac

Analytical Representations of Potential Energy Surfaces

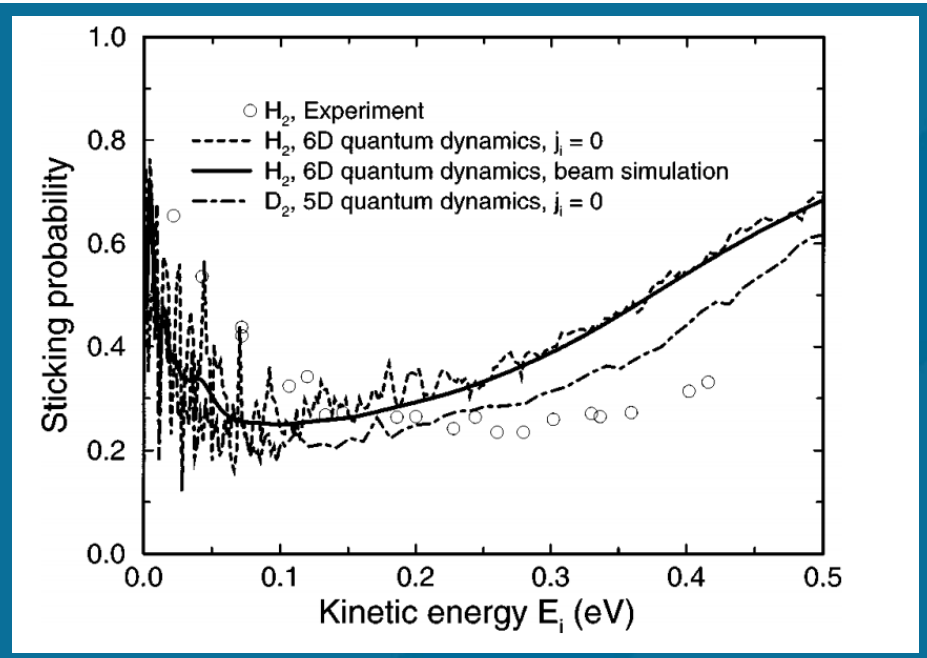

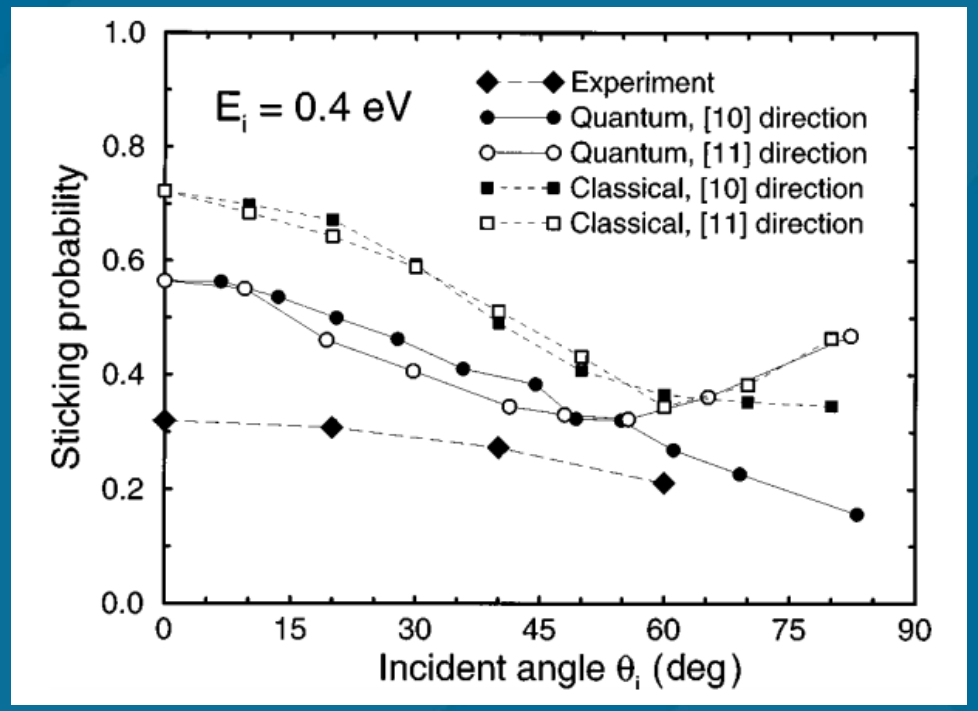

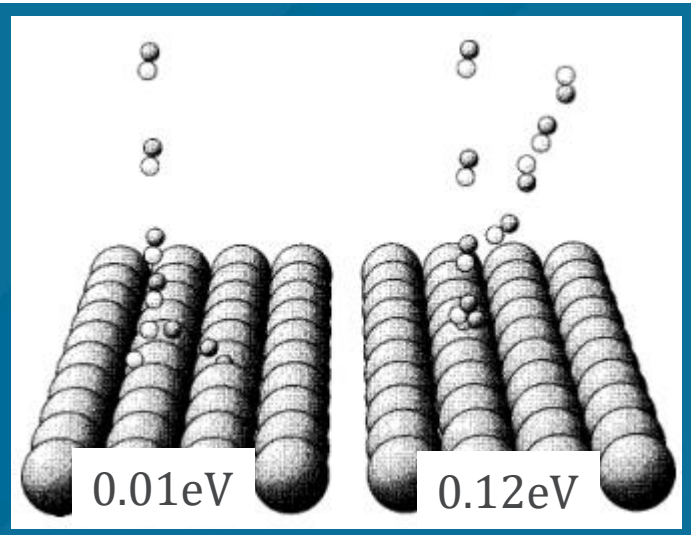

Ab initio quantum and molecular dynamics of the dissociative adsorption of hydrogen on Pd(100)

- 6D analytical model that interpolated between different calculated potential energy surfaces
- Results compared with DFT calculations

 Gross, A., Scheffler, M., *Physical Review B*, ***1997***

Analytical Representations of Potential Energy Surfaces

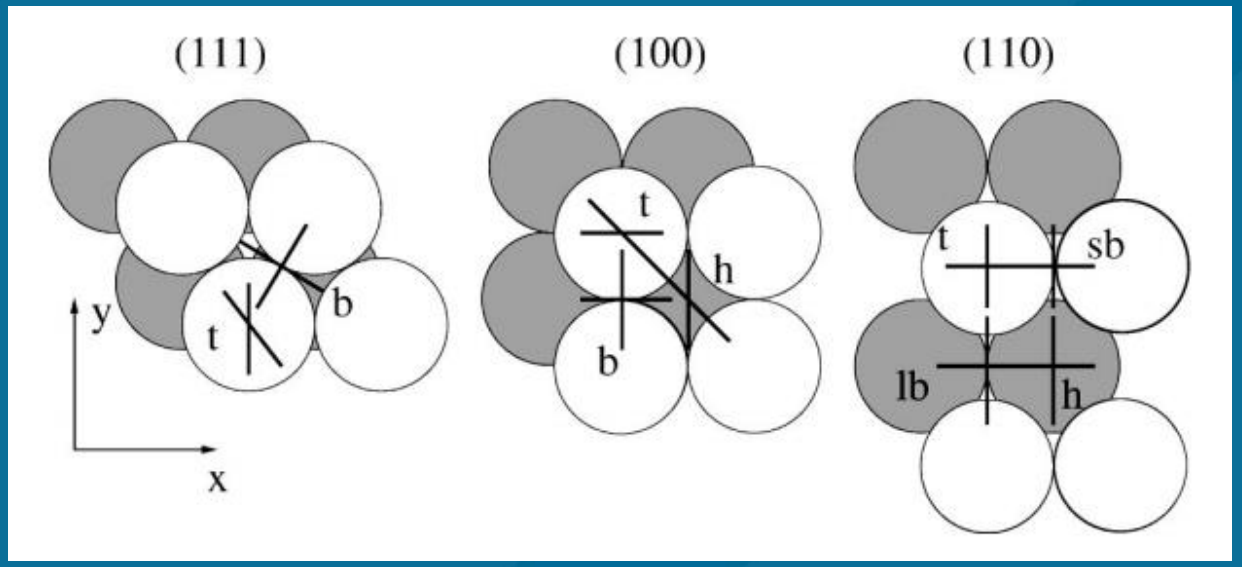

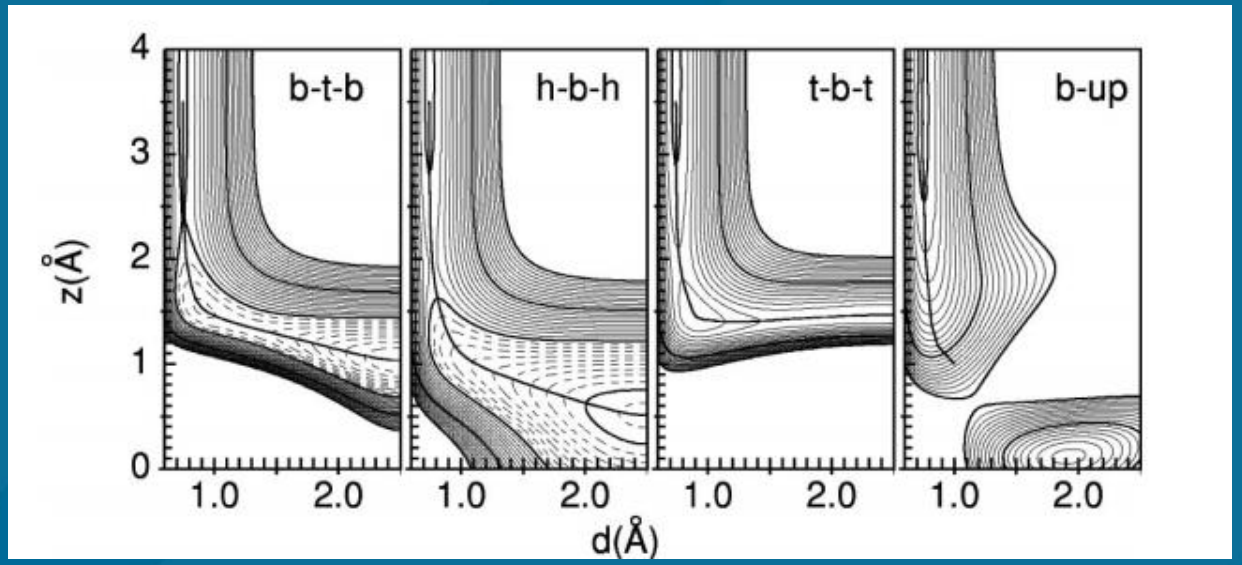

2D PES calculated for high symmetry sites and molecular orientations

Only the distance between Hydrogen atoms and the height of the atoms from the surface are varies for these 2D PESs

6D Potential obtained by interpolating between the 2D sites

Important Experimental trends captured
Deviation in surface

Inflexible and grows complex very quickly with increased problem dimensionality

 G. Wiesenekker, G. J. Kroes, E. J. Baerends, J. Chem. Phys. , ***1996***

Neural Network Representation of Potential Energy Surfaces

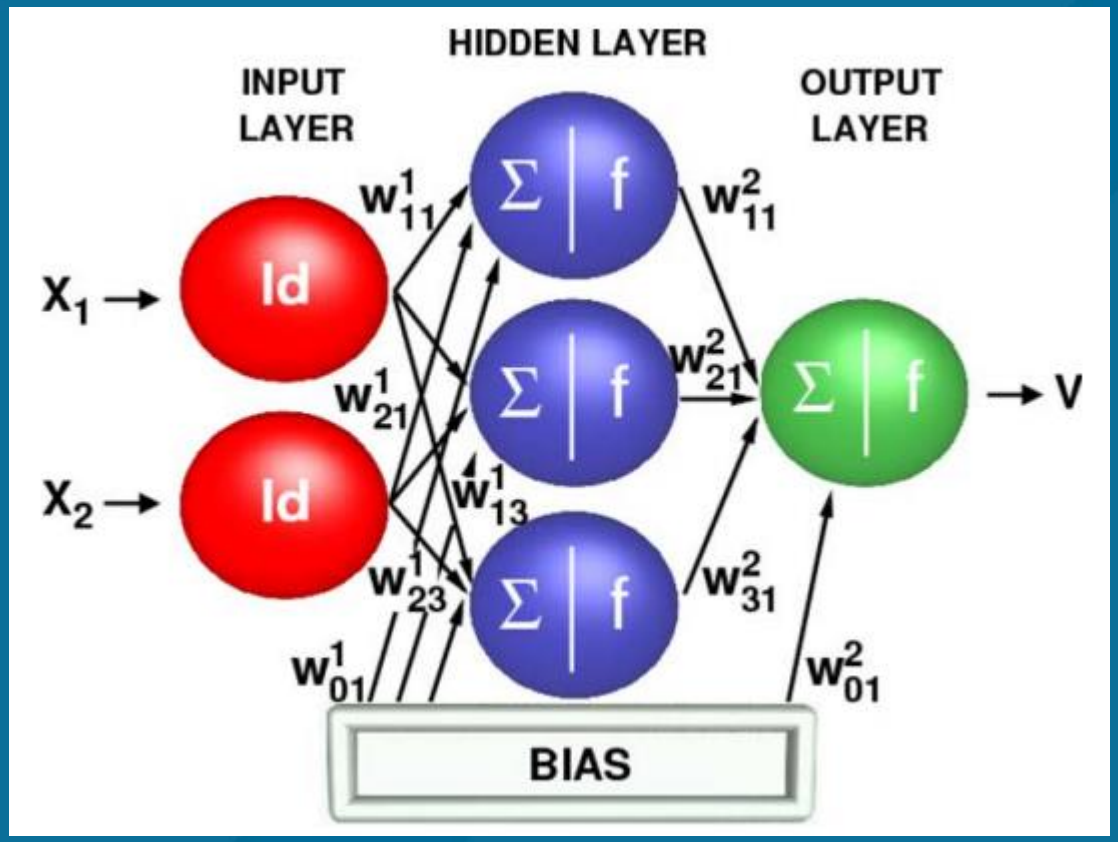

$$V_{nn}(\mathbf{x}) = f_2\left(w^2_{01} + \sum_j w^2_{j1}\, f_1\left(w^1_{0j} + \sum_{i=1}^{6} w^1_{ij} x_i\right)\right),$$

- Highly flexible, nonlinear model that can approximate any continuous function
- Artificial 'neurons' or nodes are arranged in layers and interconnected via links
- Each link is multiplied by a weight before being supplied to a new node

- Only the Input Layer and Output Layer are interacted with
  - Hidden layers not visible from the outside

- Every node is connected to every node in adjacent layers.
  - Nodes within the same layer are not connected
  - Information is only transmitted forward
  - Multilayer Feed-Forward Neural Network

Lorenz, S., Gross, A., Scheffler, M., *Chemical Physics Letters,* 2004

Neural Network Representation of Potential Energy Surfaces

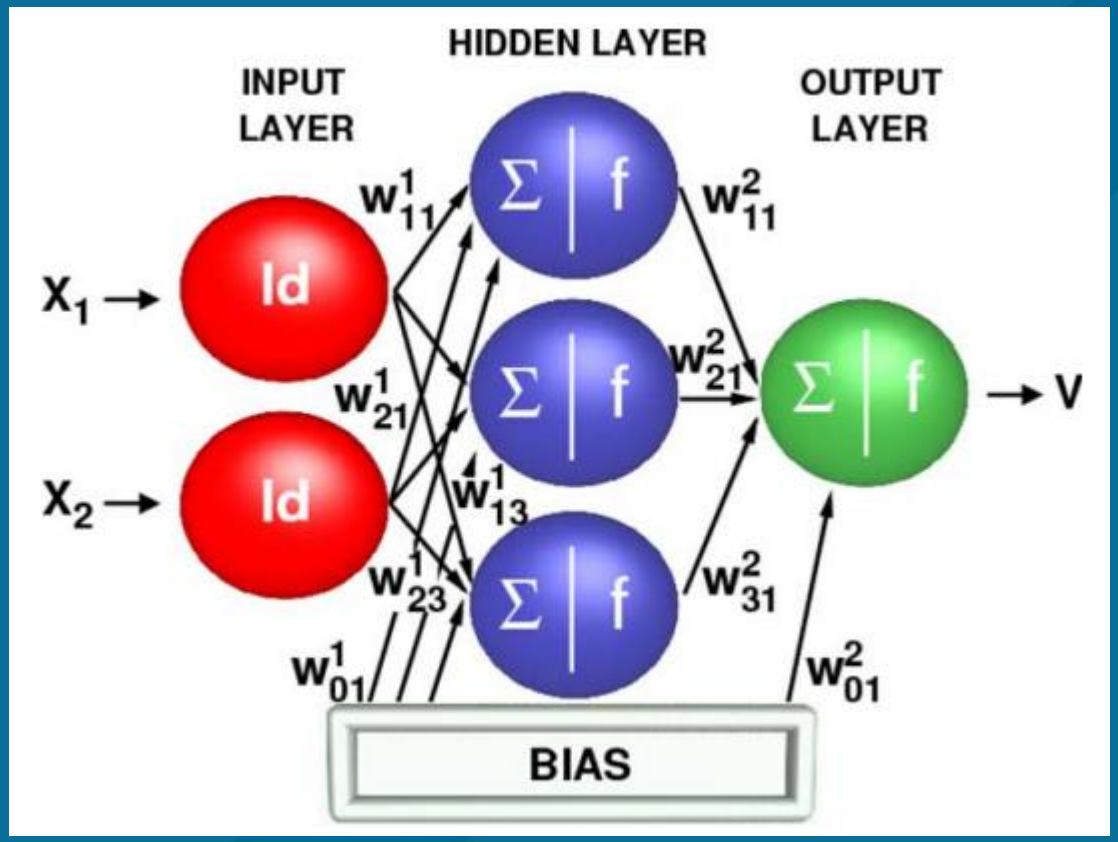

$$E(\{\mathbf{x}\}) = \sum_{i=1}^{n} u_i \left(V_{nn}(\mathbf{x}^{(i)}) - V(\mathbf{x}^{(i)})\right)^2 \Big/ \sum_{i=1}^{n} u_i,$$

- The Neural Network is minimized via the Cost Function
  - The square root of this function is the Root Mean Square Error (RMSE)
- For each new training data input, the Cost Function is minimized by adjusting the weights of the links in the neural network

- This minimization is called 'learning'
  - Typically done via gradient-based learning such as
    - Steepest Descent
    - Conjugate Gradients
    - Other algorithms
  - Global Extended Kalman Filter used in this paper
- Tested on a H_2 adhesion on Pd surface

Lorenz, S., Gross, A., Scheffler, M., *Chemical Physics Letters*, 2004

Neural Network Representation of Potential Energy Surfaces

$$x_1 = d,$$
$$x_2 = e^{Z_c/2},$$
$$x_3 = \sin^2\theta \cos 2\phi[\cos GX_c - \cos GY_c]e^{-Z_c/2},$$
$$x_4 = \sin^2\theta \cos 2\phi[\cos 2GX_c - \cos 2GY_c]e^{-Z_c/2},$$
$$x_5 = \cos^2\theta e^{-Z_c/2},$$
$$x_6 = [\cos GX_c + \cos GY_c]e^{-Z_c/2},$$
$$x_7 = [\cos 2GX_c + \cos 2GY_c]e^{-Z_c/2},$$
$$x_8 = \sin^4\theta \cos 4\phi[\cos 2GX_c + \cos 2GY_c]e^{-Z_c/2}.$$

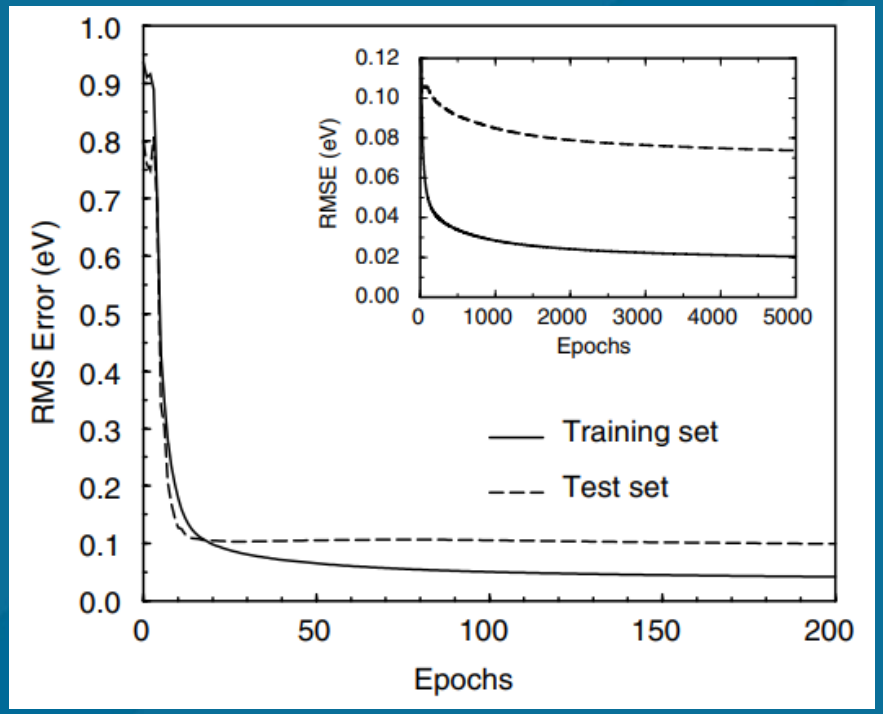

- Eight Symmetry adapted inputs chosen so all fitting is focused on the chemical dynamics of the system
  - 8-24-18-1sl neural network used

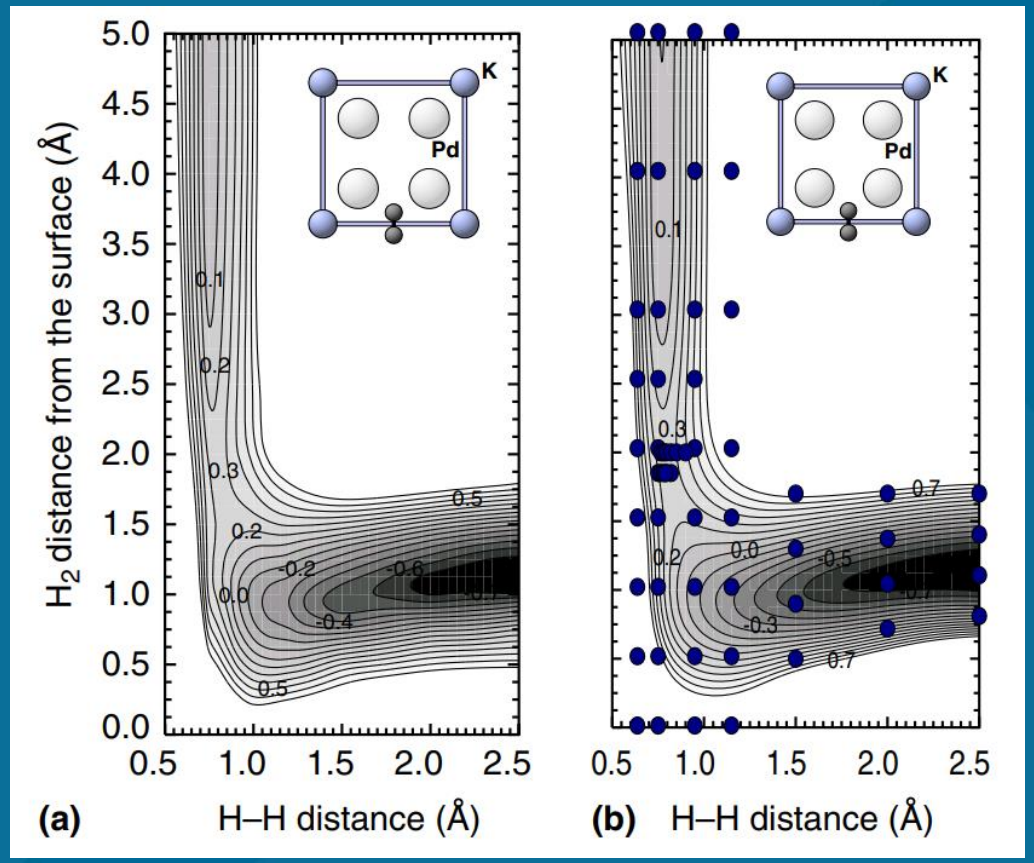

 Lorenz, S., Gross, A., Scheffler, M., *Chemical Physics Letters*, 2004

Neural Network Representation of Potential Energy Surfaces

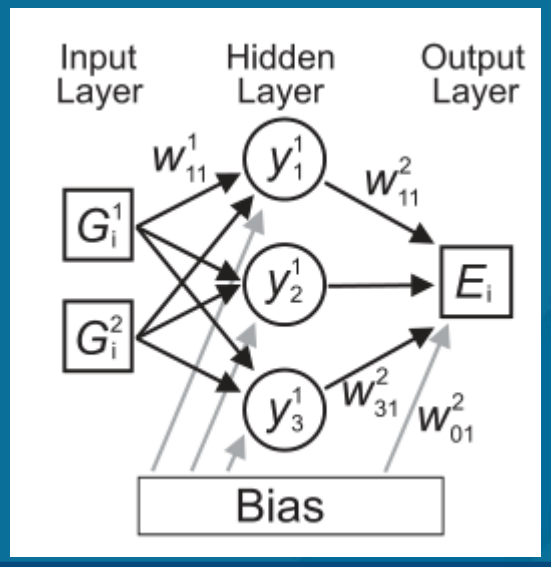

Simple Neural Network

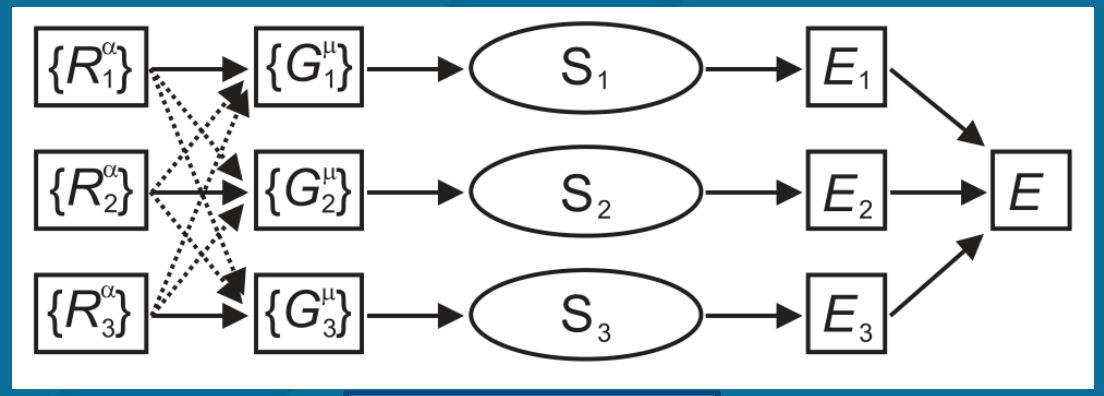

New Topology

- Simple Neural networks are nontransferable
  - They only work for the specific arrangement of input nodes they were optimized for
  - Because weights are different, configuration is not arbitrary
    - Interchanging two atomic coordinates would change the total energy even if the two atoms were the same
  - Cannot be used for a set with a different number of degrees of freedom
    - Different numbers of atoms
- A new topology must be constructed to address these issues
  - Represent total energy as a sum of each atomic energy
  - Transform coordinates of all atoms with symmetry functions to create local environments
- Each atom's environment is fed into a simple NN

 Jörg Behler and Michele Parrinello, *Phys. Rev. Lett.*, 2007

Neural Network Representation of Potential Energy Surfaces

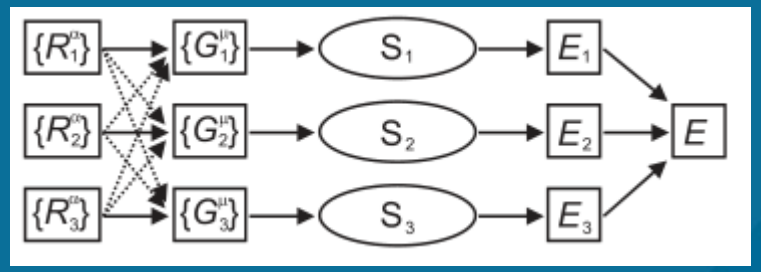

$$G_i^1 = \sum_{j \neq i}^{\text{all}} e^{-\eta(R_{ij}-R_s)^2} f_c(R_{ij}).$$

Radial Symmetry Function

$$G_i^2 = 2^{1-\zeta} \sum_{j,k \neq i}^{\text{all}} (1 + \lambda \cos\theta_{ijk})^\zeta \times e^{-\eta(R_{ij}^2+R_{ik}^2+R_{jk}^2)} f_c(R_{ij}) f_c(R_{ik}) f_c(R_{jk}),$$

Angular Symmetry Function

- Symmetry Functions convert the positions of all atoms to local environments for each atom
  - Two structures with different energies must yield different symmetry function values
  - Identical structures must yield the same values
  - Must be invariant with respect to translation and rotation
  - Must not be coordination dependents, as coordination can change during simulation
  - Similar to empirical potentials, but describes only structure and not energy

- G1 – Radial Distribution, Sum of Gaussians
- G2 – Angular Distribution, sum of cosines centered on *I*

  - Any basis that sufficiently describes atomic environment works

 Jörg Behler and Michele Parrinello, *Phys. Rev. Lett.,* 2007

Neural Network Representation of Potential Energy Surfaces

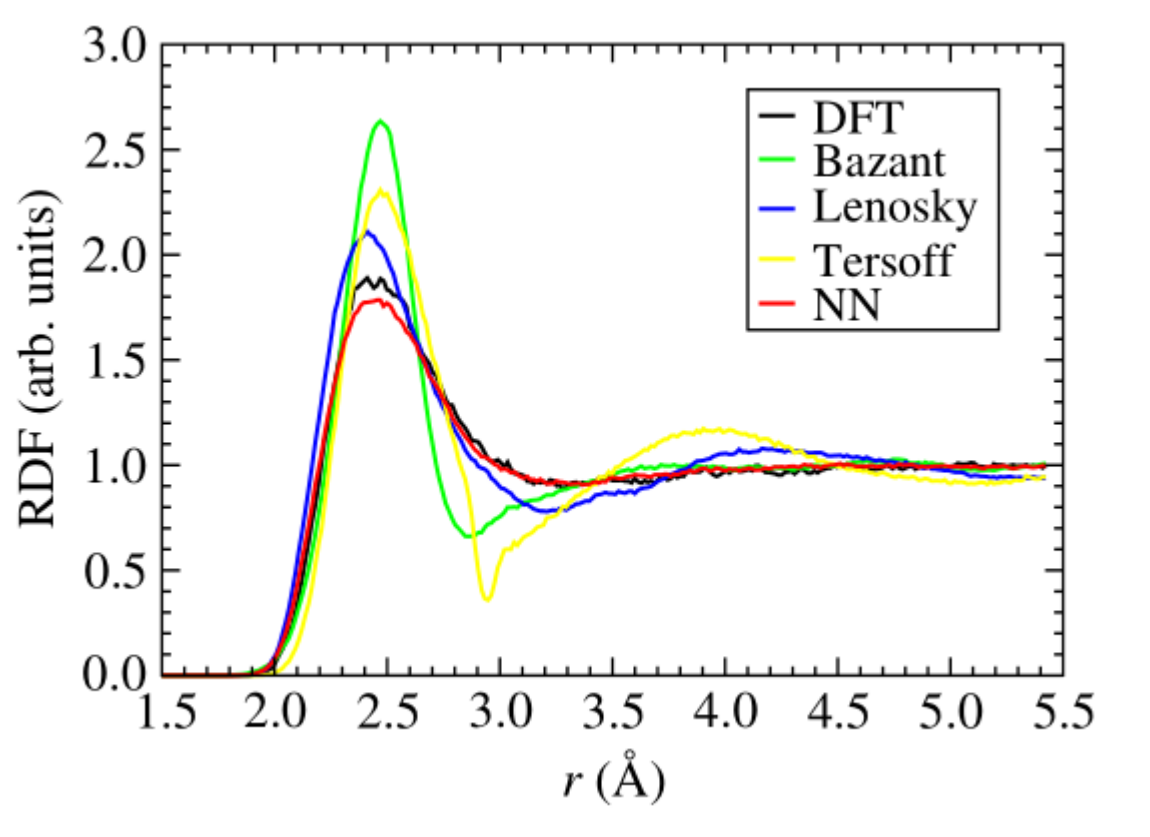

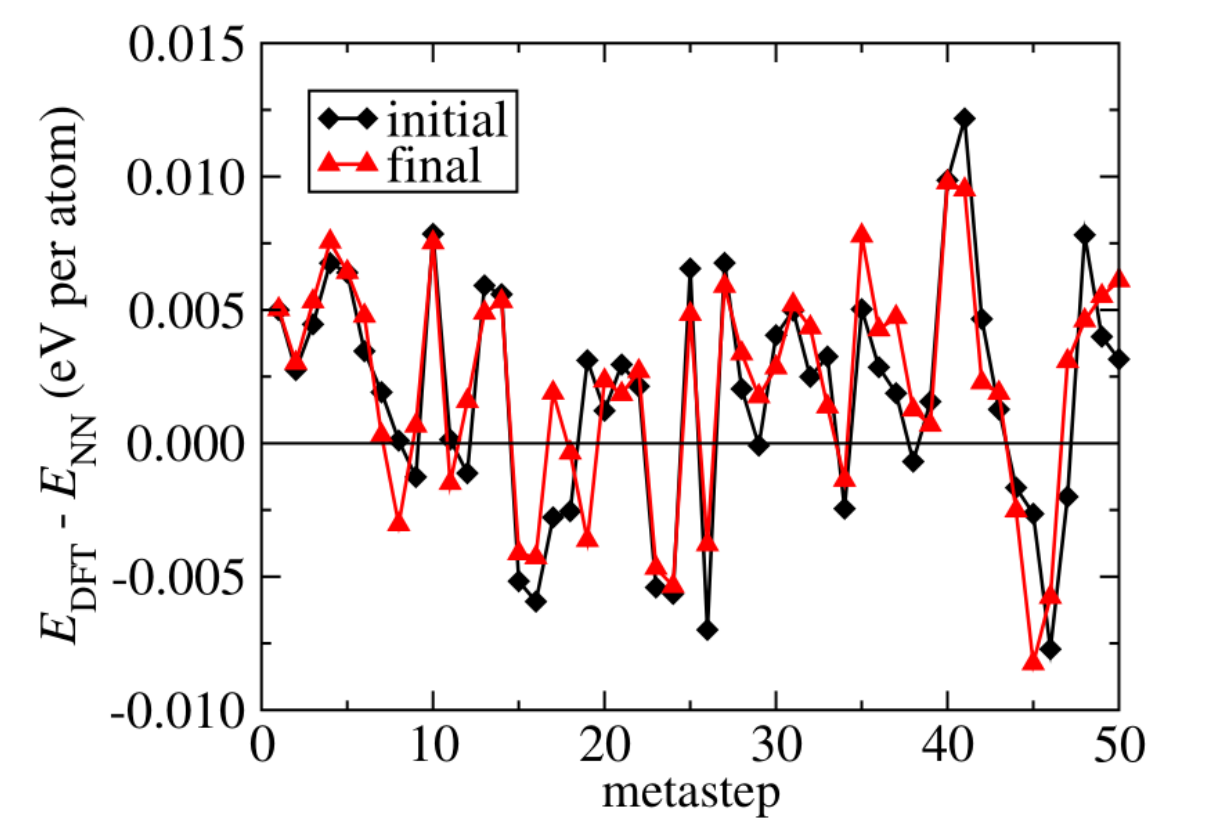

 Jörg Behler and Michele Parrinello, *Phys. Rev. Lett.,* 2007

A Machine learning based interatomic potential for amorphous carbon

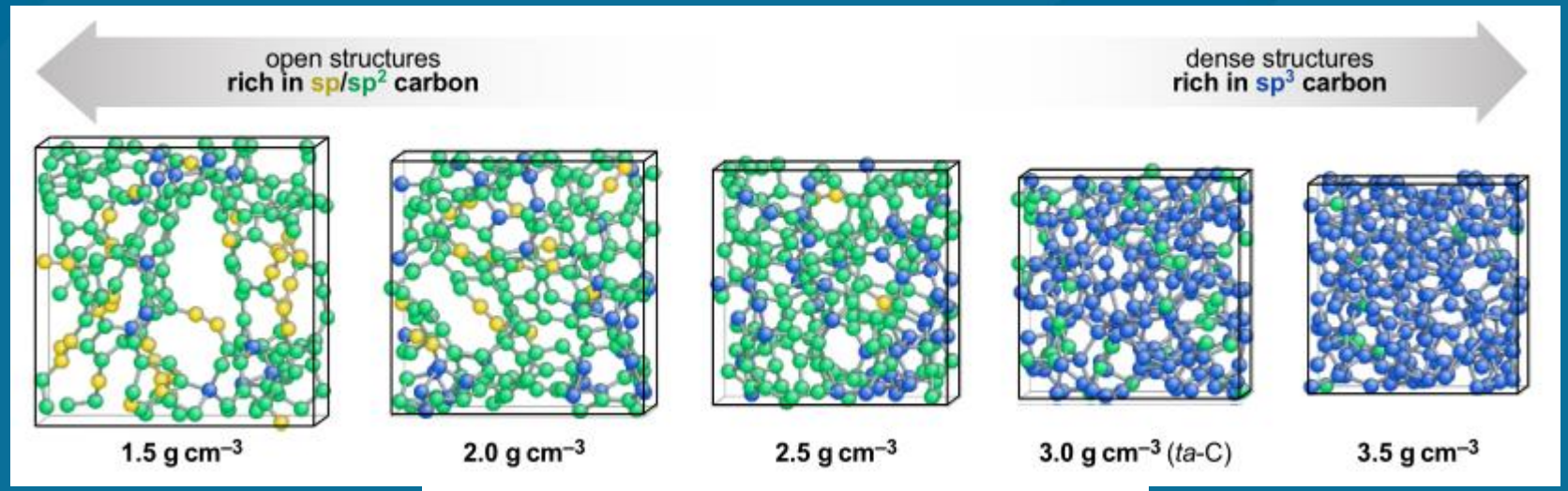

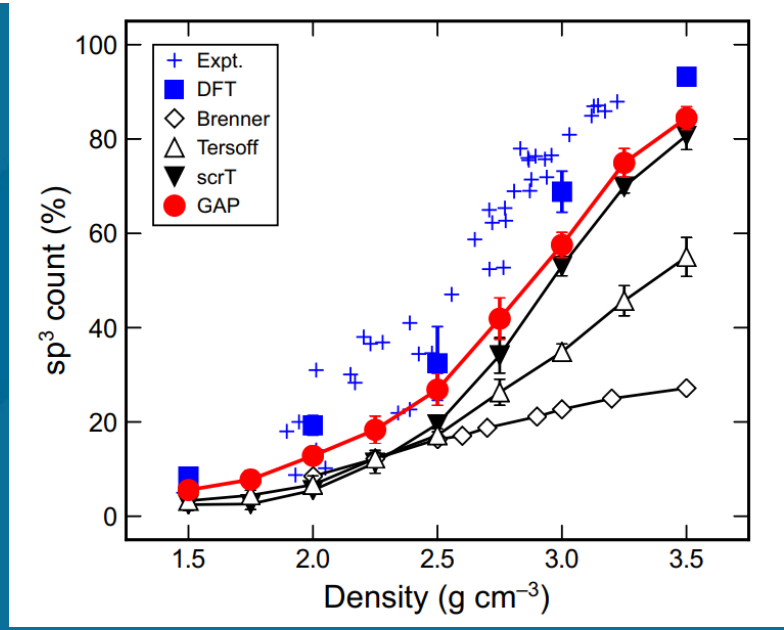

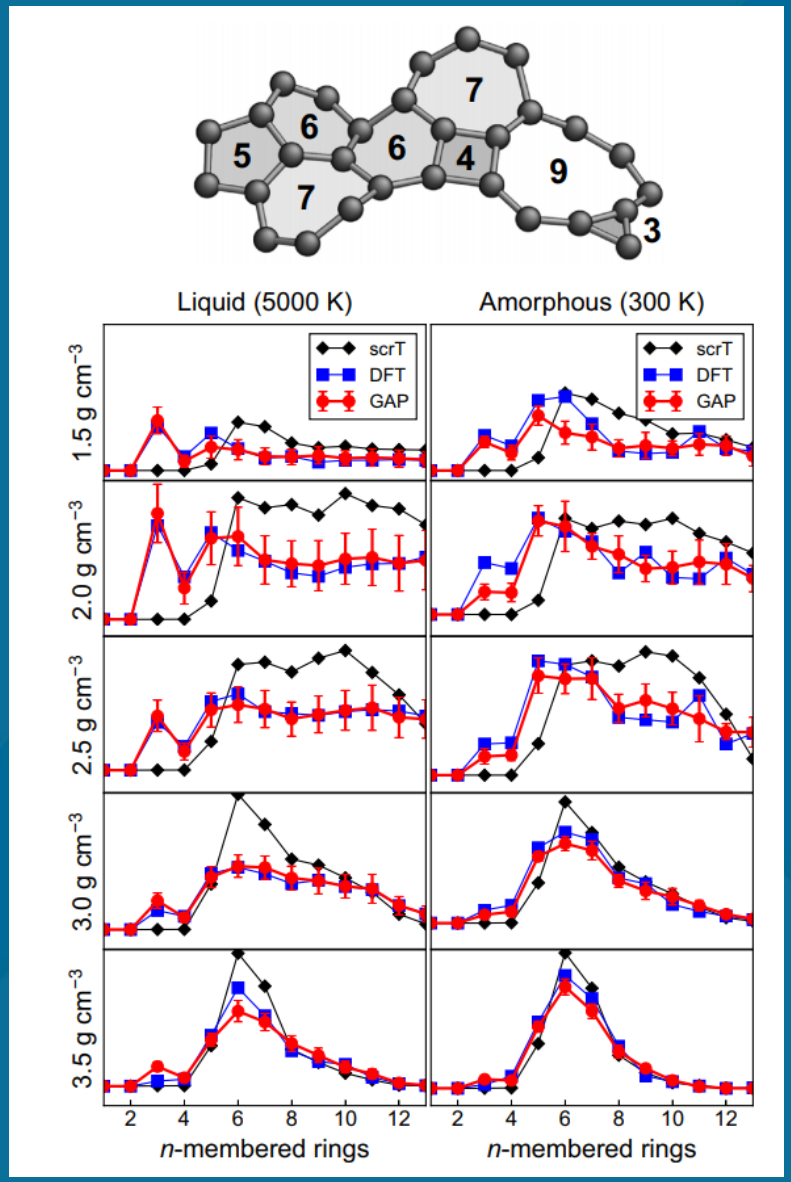

 Deringer, V., Csyani, G., *Physical Review B*, 2017

Neural Network Potentials for Multicomponent Systems

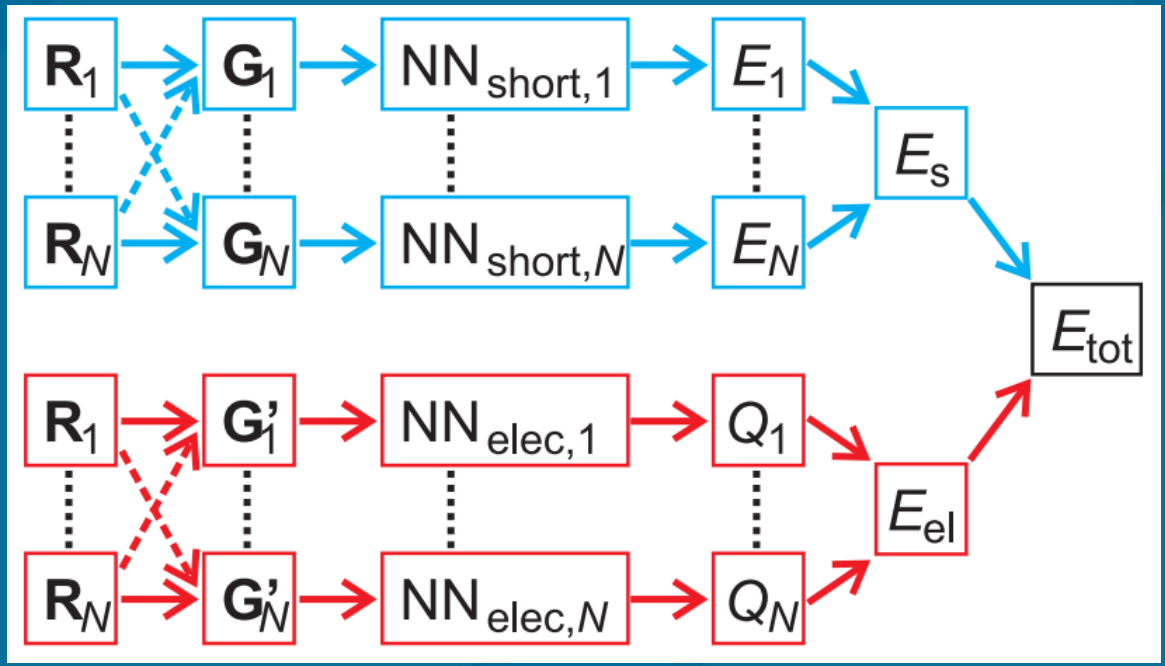

	DFT		NN	
	E_{coh} (eV)	Lattice	E_{coh} (eV)	Lattice
Wurtzite	7.057	$a = 3.278$ Å	7.054	$a = 3.278$ Å
		$c/a = 1.614$		$c/a = 1.614$
		$u = 0.379$		$u = 0.379$
Zinc blende	7.043	$a = 4.616$ Å	7.041	$a = 4.612$ Å
NaCl	6.747	$a = 4.328$ Å	6.745	$a = 4.344$ Å
CsCl	5.584	$a = 2.688$ Å	5.588	$a = 2.680$ Å

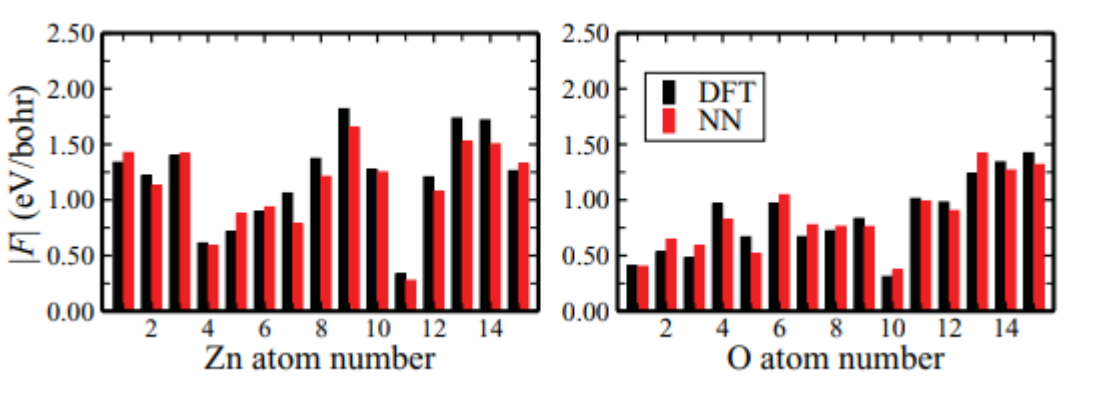

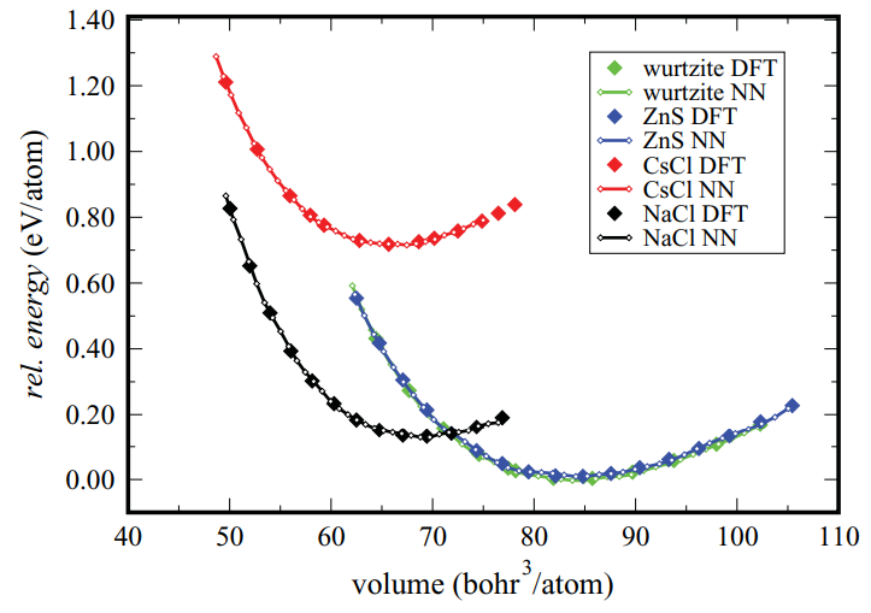

 Artrith, N., Morawietz, T., Behler, J., *Physical Review B*, 2011

Active Learning Machine Potentials – Structure Prediction

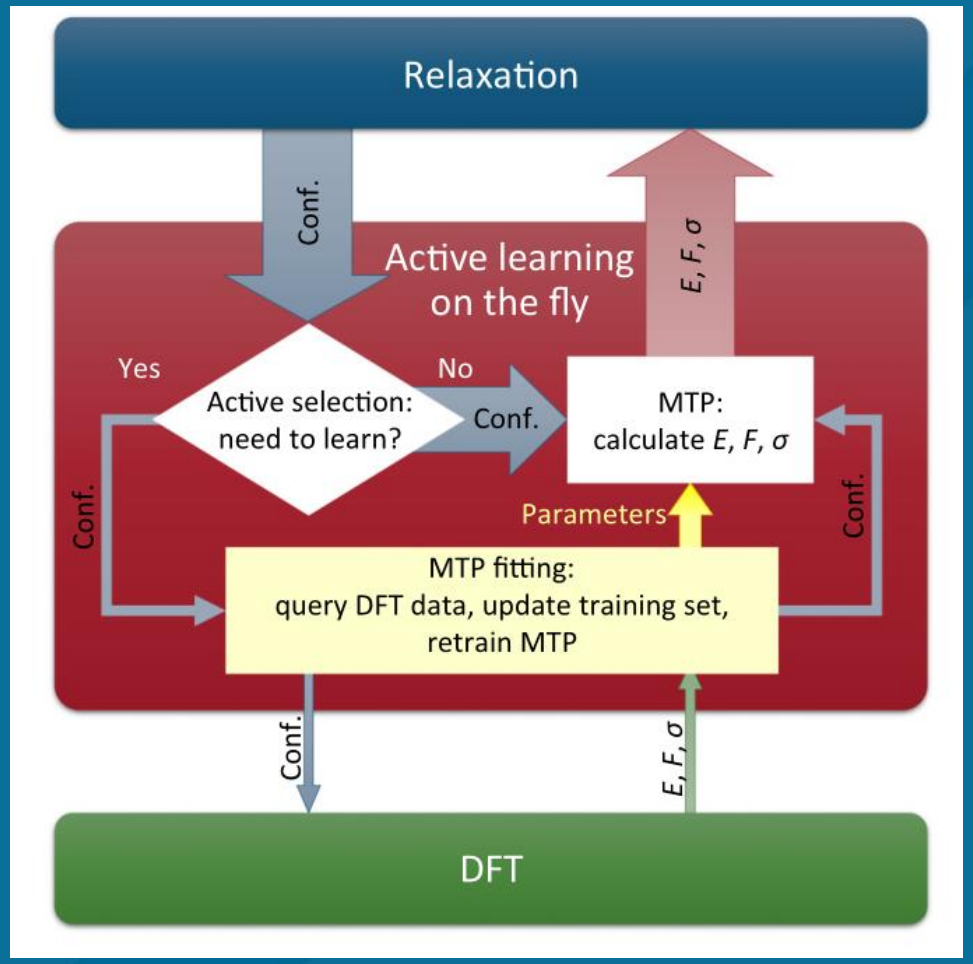

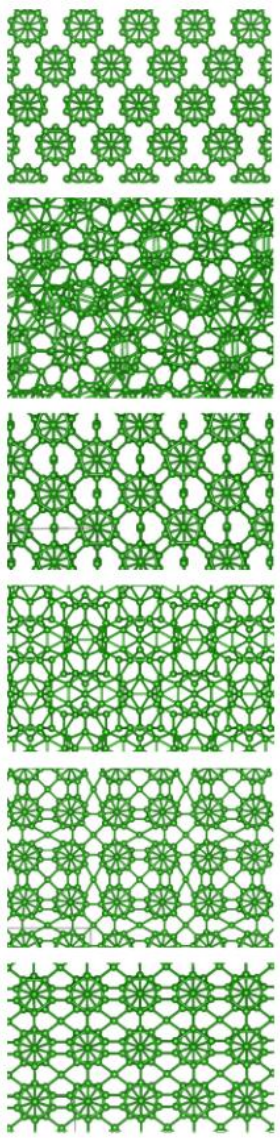

α-boron
E^{DFT}= −6.706 eV/atom
Atoms: 12,
Space group: *R*-3*m*,
Core-hours: 10^3 AL-MTP vs. $3{\cdot}10^3$ DFT
$|E^{DFT} - E^{MTP}|$ = 28.6 meV/atom

β-boron approximant
E^{DFT} = −6.704 eV/atom,
Atoms: 106,
Space group: *P*1,
Core-hours: $7{\cdot}10^3$ AL-MTP vs. $6.6{\cdot}10^7$ DFT
$|E^{DFT} - E^{MTP}|$ = 10.1 meV/atom

γ-boron
E^{DFT} = −6.678 eV/atom
Atoms: 28,
Space group: *Pnnm*,
Core-hours: $2{\cdot}10^3$ AL-MTP vs. $2.5{\cdot}10^4$ DFT
$|E^{DFT} - E^{MTP}|$ = 58.1 meV/atom

E^{DFT} = −6.667 eV/atom,
Atoms: 54,
Space group: *Im*-3,
Core-hours: $3{\cdot}10^3$ AL-MTP vs. $3.5{\cdot}10^5$ DFT
$|E^{DFT} - E^{MTP}|$ = 7.3 meV/atom

E^{DFT} = −6.667 eV/atom,
Atoms: 52,
Space group: *P*-42*m*,
Core-hours: $3{\cdot}10^3$ AL-MTP vs. $3.2{\cdot}10^5$ DFT
$|E^{DFT} - E^{MTP}|$ = 37.3 meV/atom

E^{DFT} = −6.665 eV/atom,
Atoms: 26,
Space group: *Cccm*,
Core-hours: $2{\cdot}10^3$ AL-MTP vs. $2.1{\cdot}10^4$ DFT
$|E^{DFT} - E^{MTP}|$ = 13.6 meV/atom

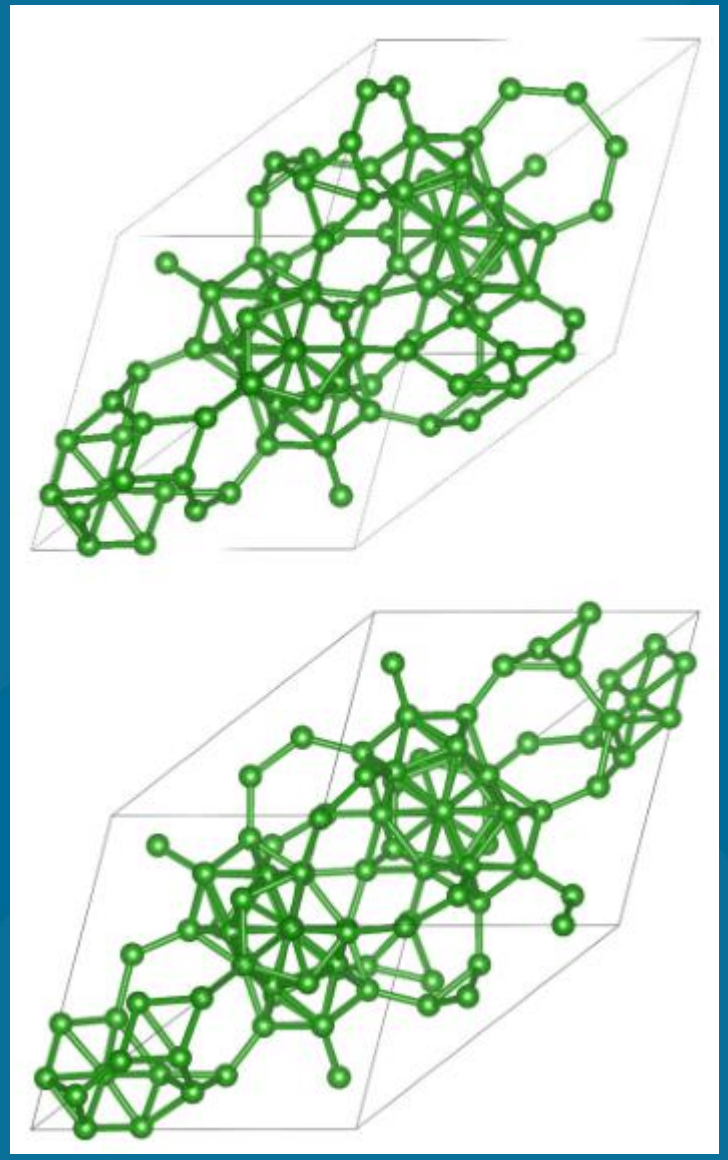

 Podryabinkin, Evgeny V. et al., Phys. Rev. B, 2019

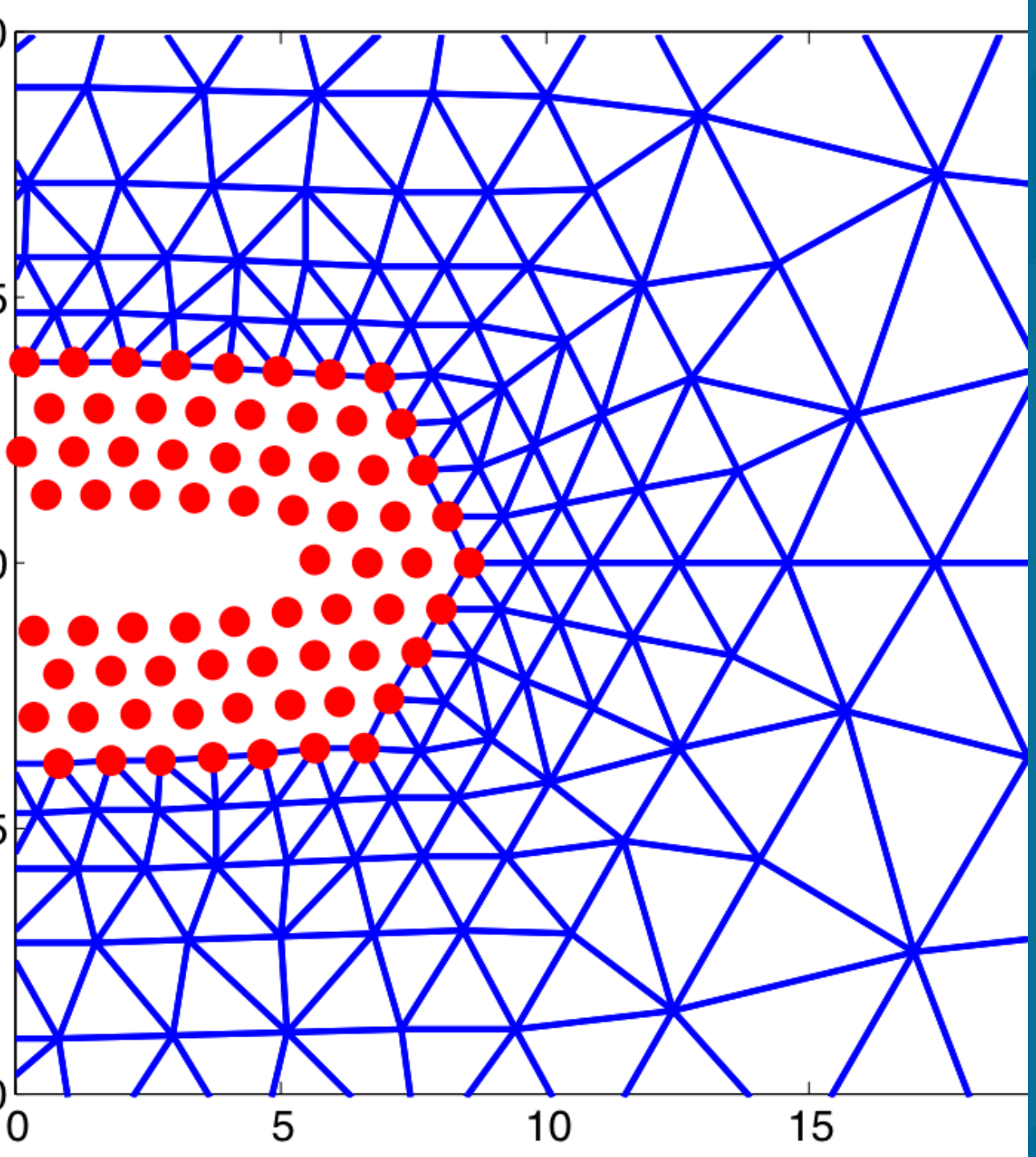

Multiscale Modeling

Bridging Length and Time Scales

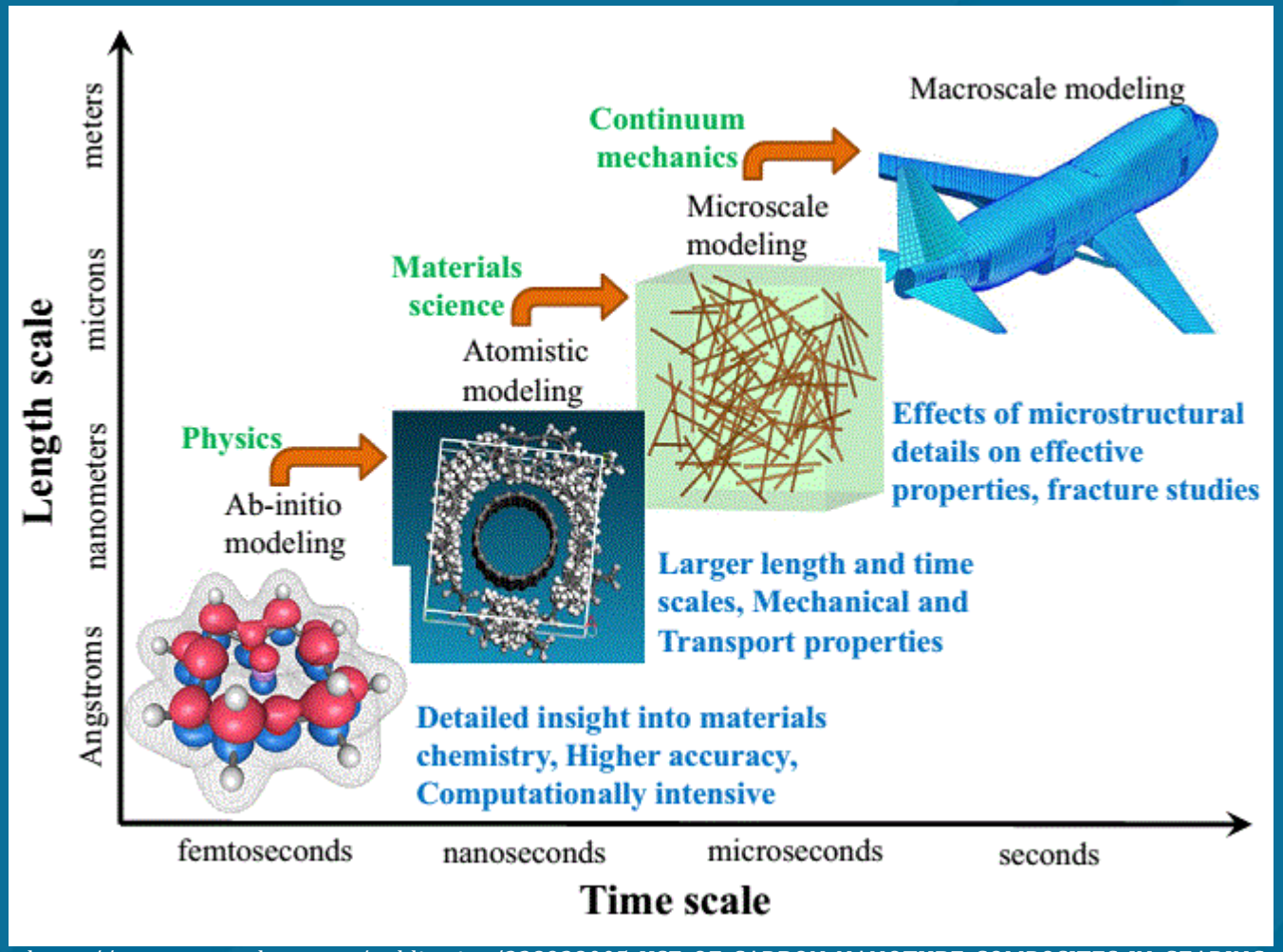

https://www.researchgate.net/publication/328928005_USE_OF_CARBON_NANOTUBE_COMPOSITES_IN_GEARING

- Ab intio calculations of DFT and Molecular Dynamics are still extremely limited in the length and time scales they can simulate with currency computational power
- Multiscale modeling attempts to bridge the length and time scales such that simulations can approach the scale of real experiments or beyond

Quasicontinuum Method – Atomistic Simulations in FEA

Cauchy-Born Rule

In a crystalline solid subject to a small strain, the positions of the atoms within the crystal lattice follow the overall strain of the medium

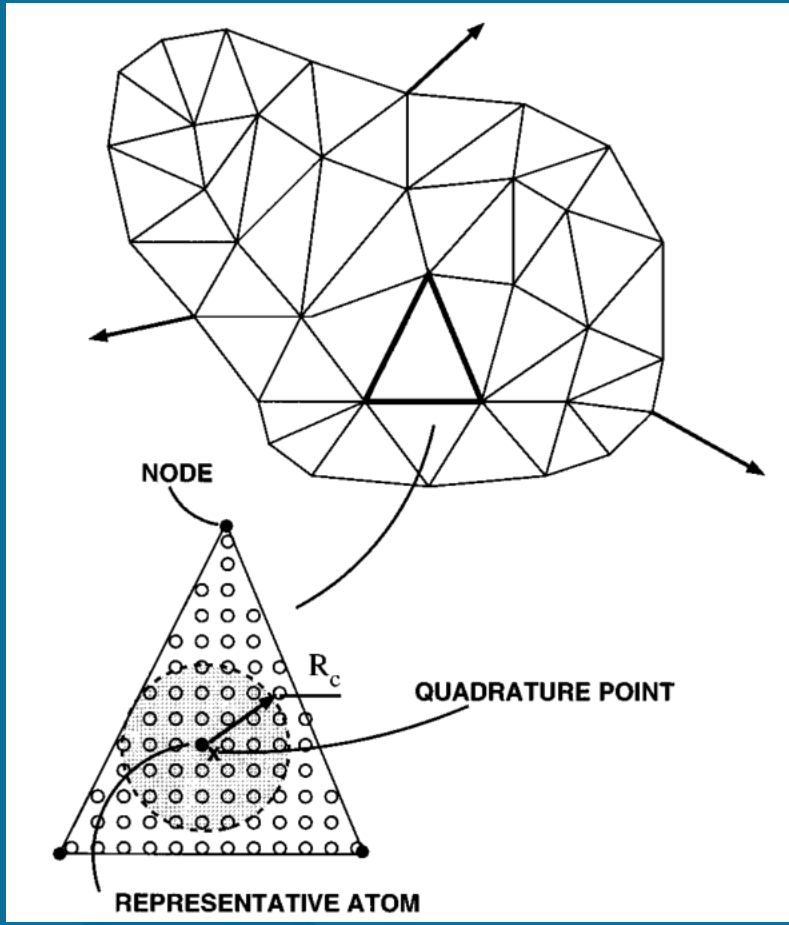

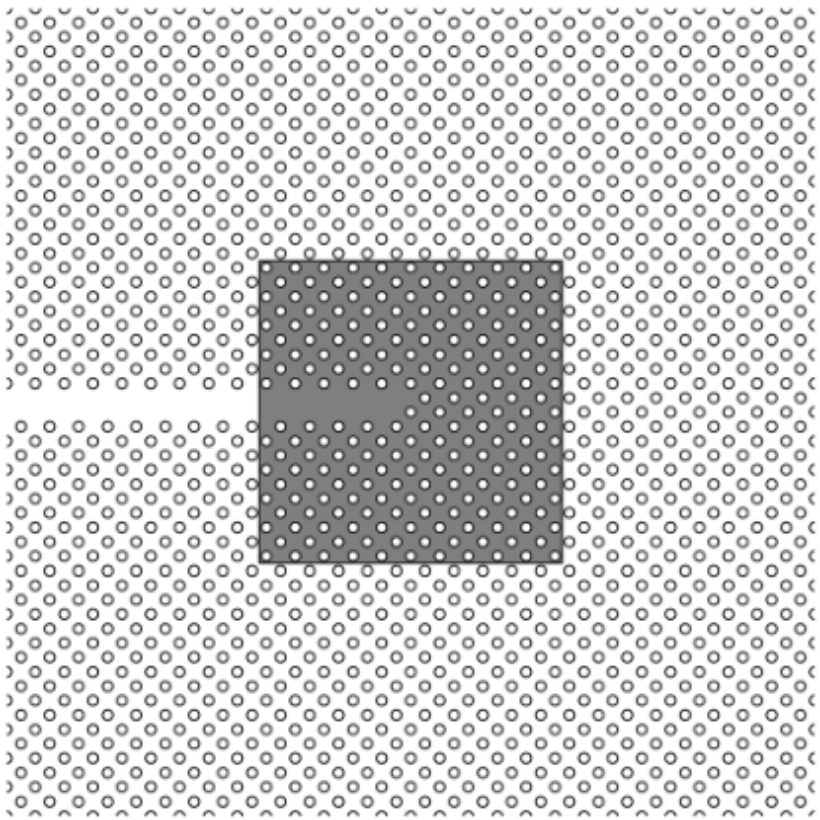

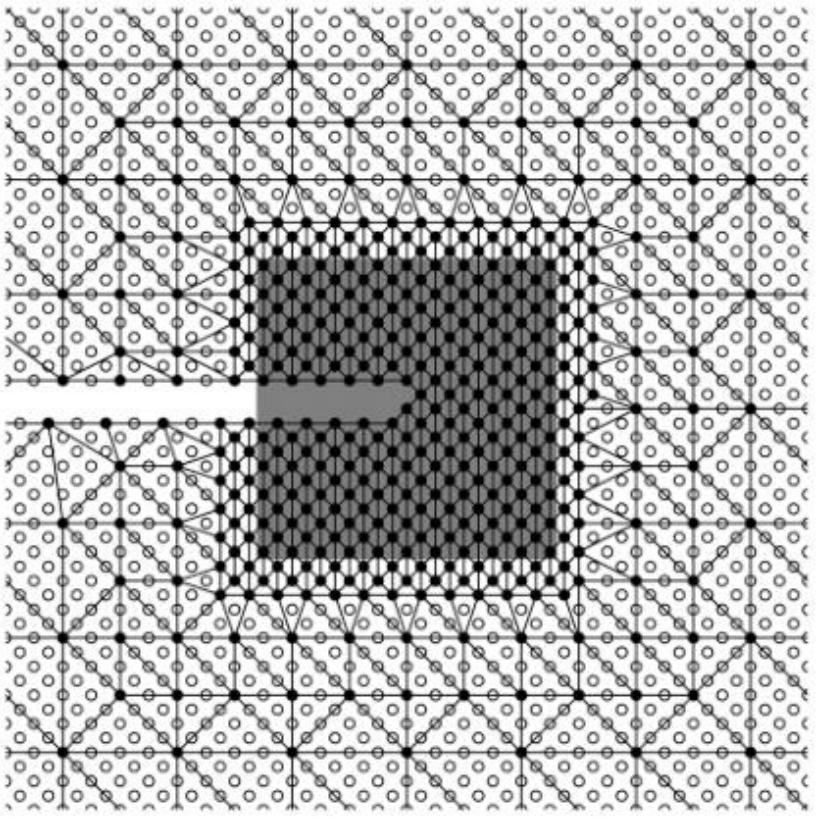

 E. B. Tadmor , M. Ortiz & R. Phillips, *Philosophical Magazine A,* 1996

Quasicontinuum Method – Testing Edge Cases

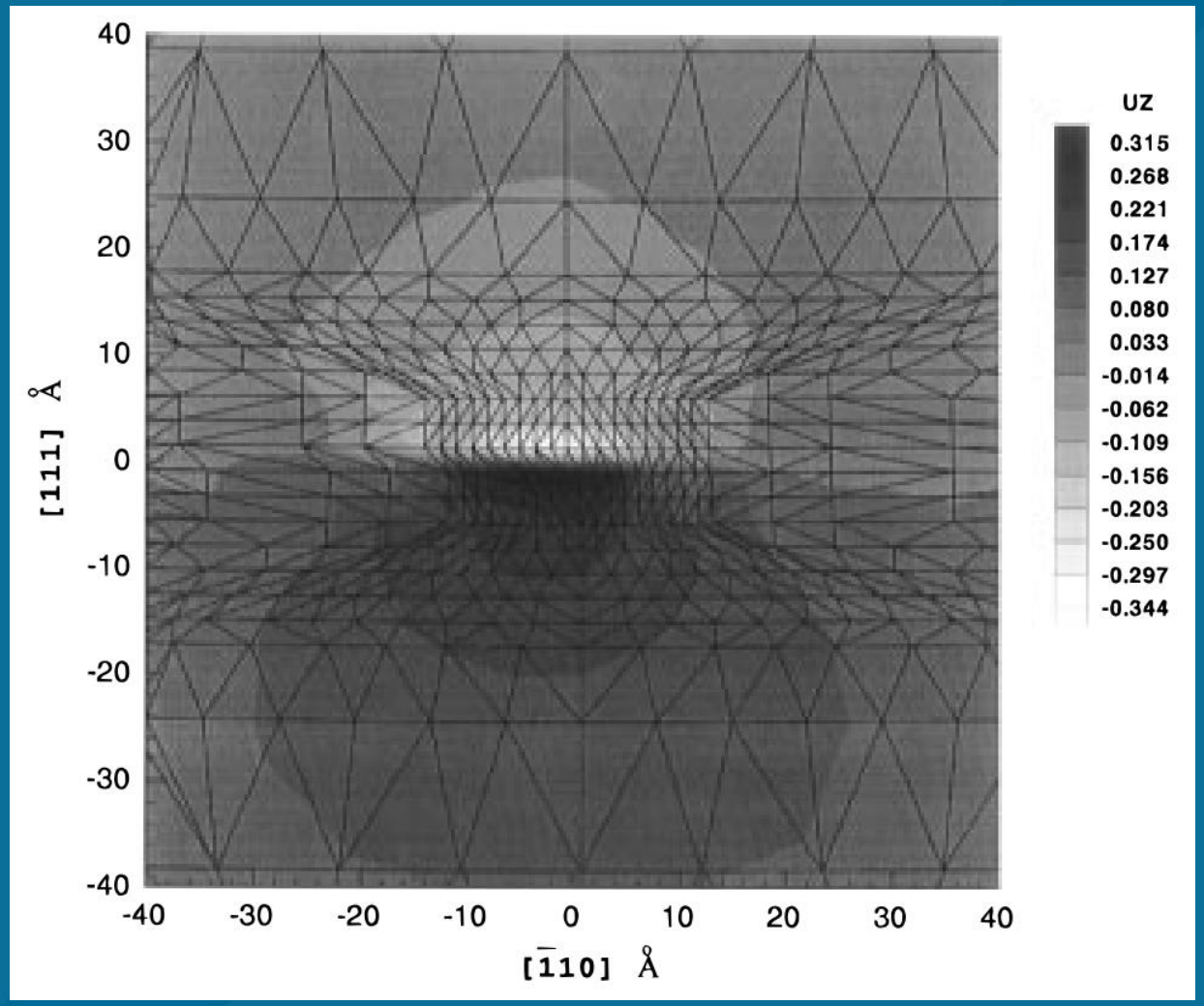

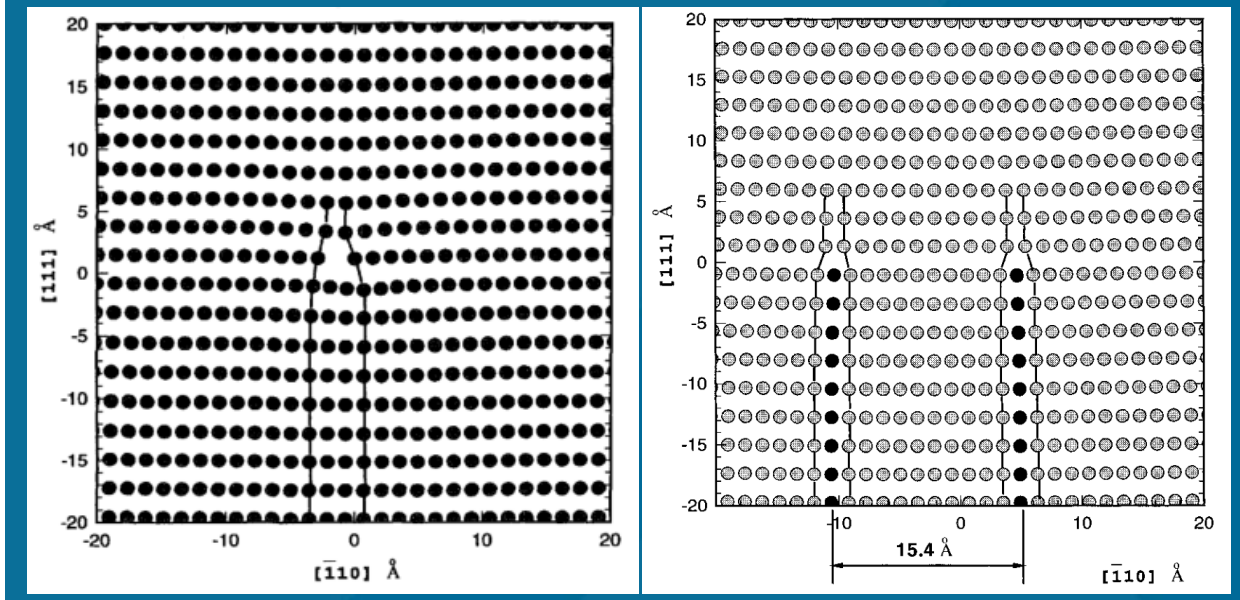

 E. B. Tadmor , M. Ortiz & R. Phillips, *Philosophical Magazine A,* 1996

Quasicontinuum Method – Modeling Nanoindentation

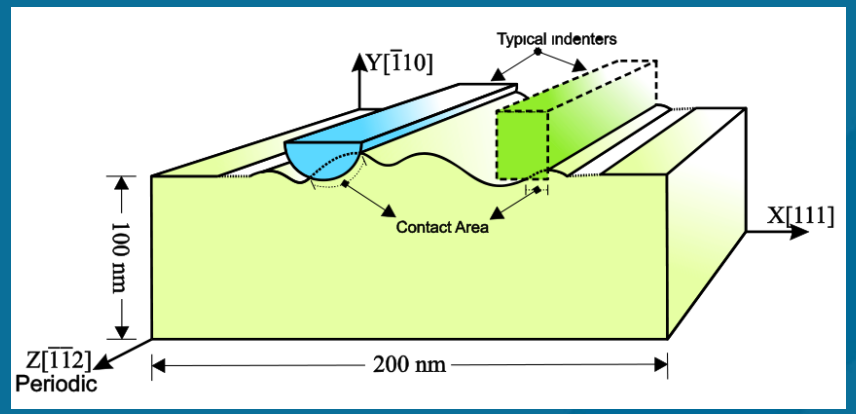

200 x 100 nm Cu FCC Crystal

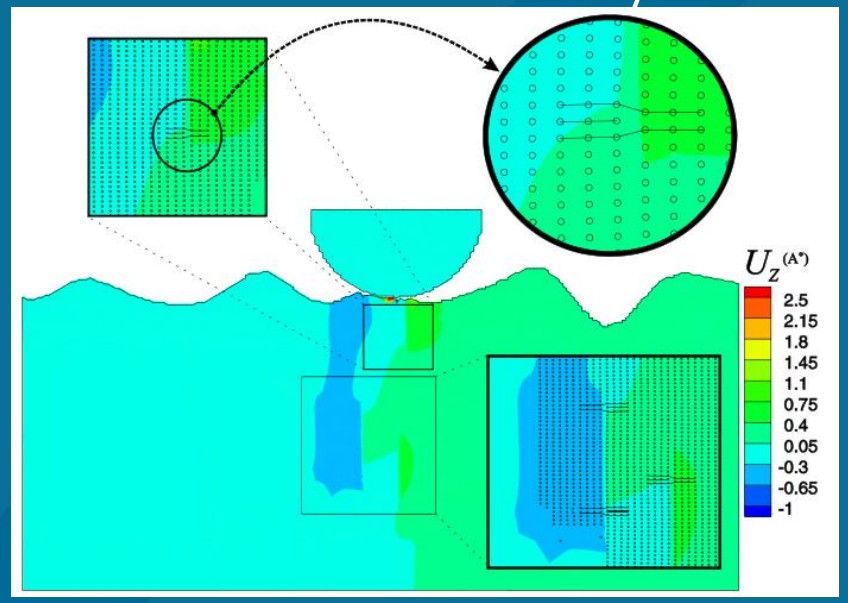

Z displacement for a R=6.5A indenter

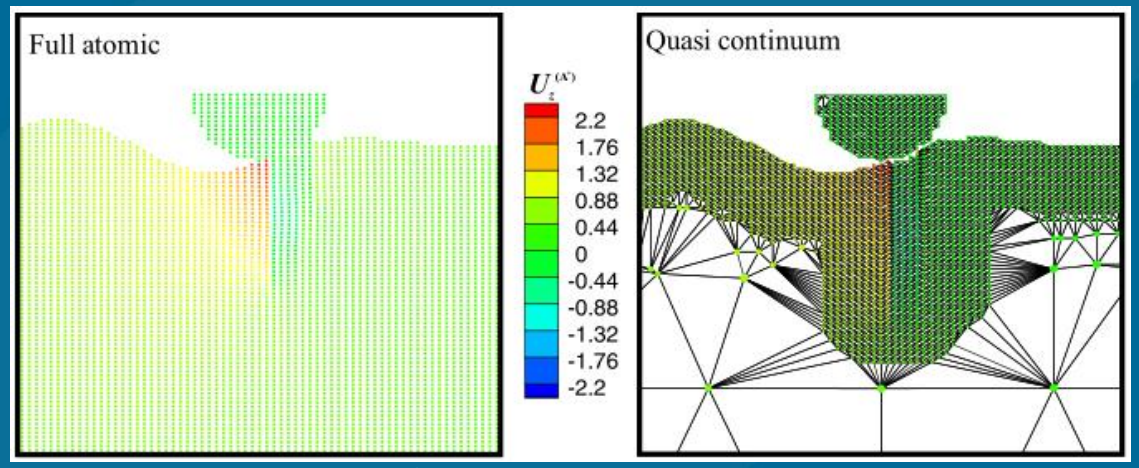

Out of plane displacement

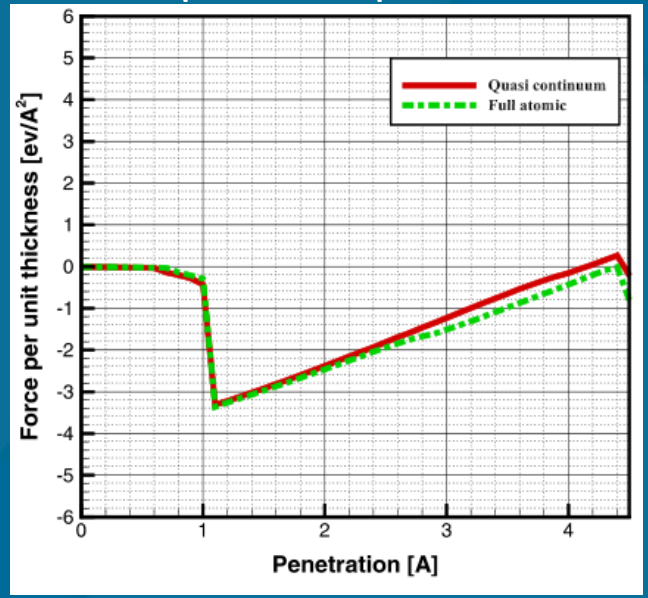

Load Penetration Curves

Moslemzadeh, H., Alizadeh, O. & Mohammadi, S., *Meccanica,* (2019)

Quasicontinuum Method – Nanowelding Analysis

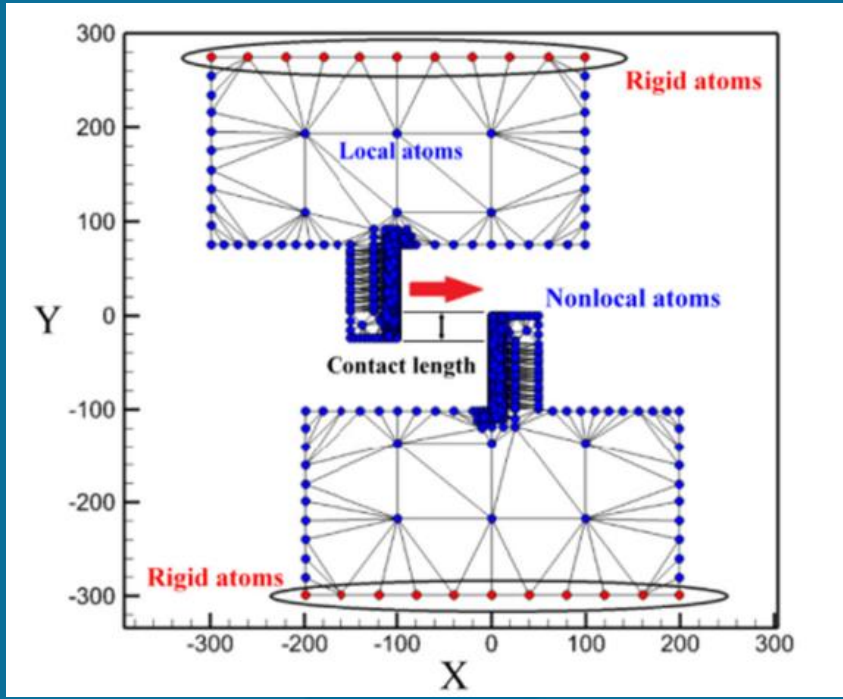

Schematic of the QC mesh

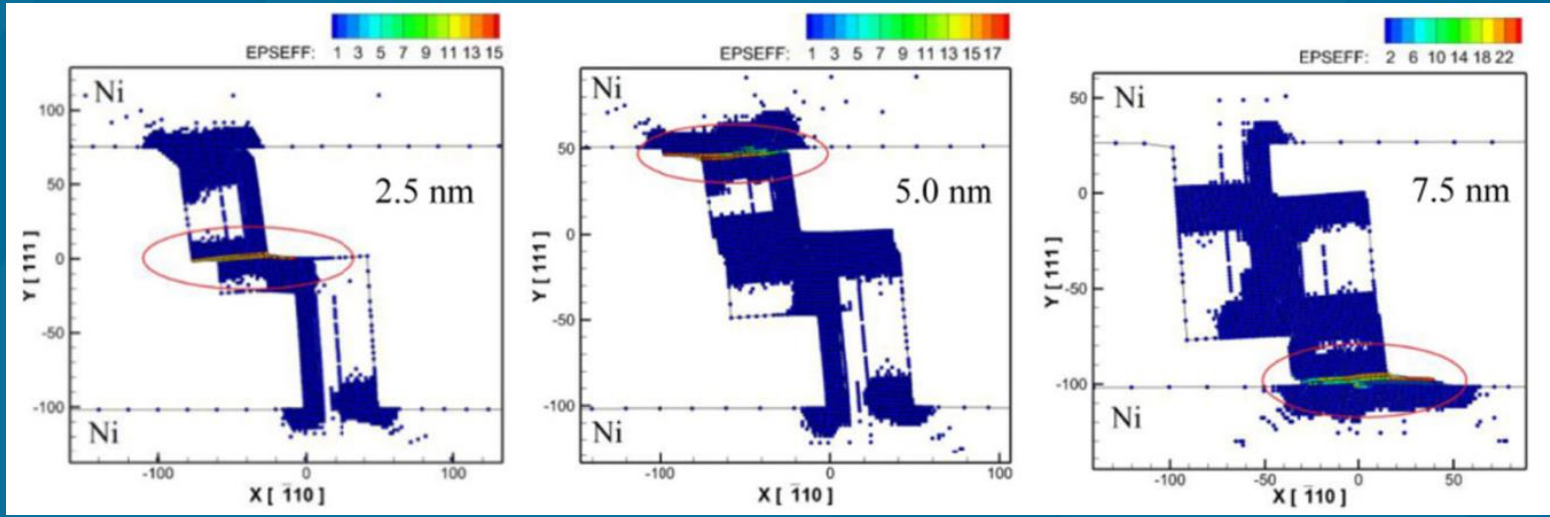

Strain may occur at roots of the weld instead of at the contact points

 Wu, CD., Fang, TH. & Lin, YJ., *J Mol Model* (2018)

Finite Temperature Quasicontinuum

$$\tilde{\mathcal{H}}^{\mathrm{at}}(\boldsymbol{q}^{\mathrm{at}}, \boldsymbol{p}^{\mathrm{at}}, T) = \tilde{\mathcal{V}}^{\mathrm{at}}(\boldsymbol{q}^{\mathrm{at}}, T) + \mathcal{K}^{\mathrm{at}}(\boldsymbol{p}^{\mathrm{at}}, T)$$

$$\Psi^{\mathrm{c}}_{\mathrm{LH}}(\boldsymbol{q}^{\mathrm{at}}, \overset{*}{\boldsymbol{q}}^{\mathrm{c}}, T) = \mathcal{V}(\boldsymbol{q}^{\mathrm{at}}, \overset{*}{\boldsymbol{q}}^{\mathrm{c}}) + \frac{k_B T}{2} \sum_{i=1}^{N_{\mathrm{c}}} \ln \left[\frac{h_q^6 \det \boldsymbol{\Phi}^{\mathrm{c}}_{ii}(\boldsymbol{q}^{\mathrm{at}}, \overset{*}{\boldsymbol{q}}^{\mathrm{c}})}{(2\pi k_B T)^3} \right]$$

$$\tilde{\mathcal{V}}^{\mathrm{at}}(\boldsymbol{q}^{\mathrm{at}}, T) = \min_{\overset{*}{\boldsymbol{q}}^{\mathrm{c}}} \Psi^{\mathrm{c}}_{\mathrm{LH}}(\boldsymbol{q}^{\mathrm{at}}, \overset{*}{\boldsymbol{q}}^{\mathrm{c}}, T)$$

$$\mathcal{K}^{\mathrm{at}}(\boldsymbol{p}^{\mathrm{at}}, T) = \sum_{i=1}^{N_{\mathrm{at}}} \frac{\left\| \boldsymbol{p}_i^{\mathrm{at}} \right\|^2}{2 m_i^{\mathrm{at}}} - \frac{3 k_B T}{2} \sum_{j=1}^{N_{\mathrm{c}}} \ln \frac{2\pi k_B T m_j^{\mathrm{c}}}{h_p^2}$$

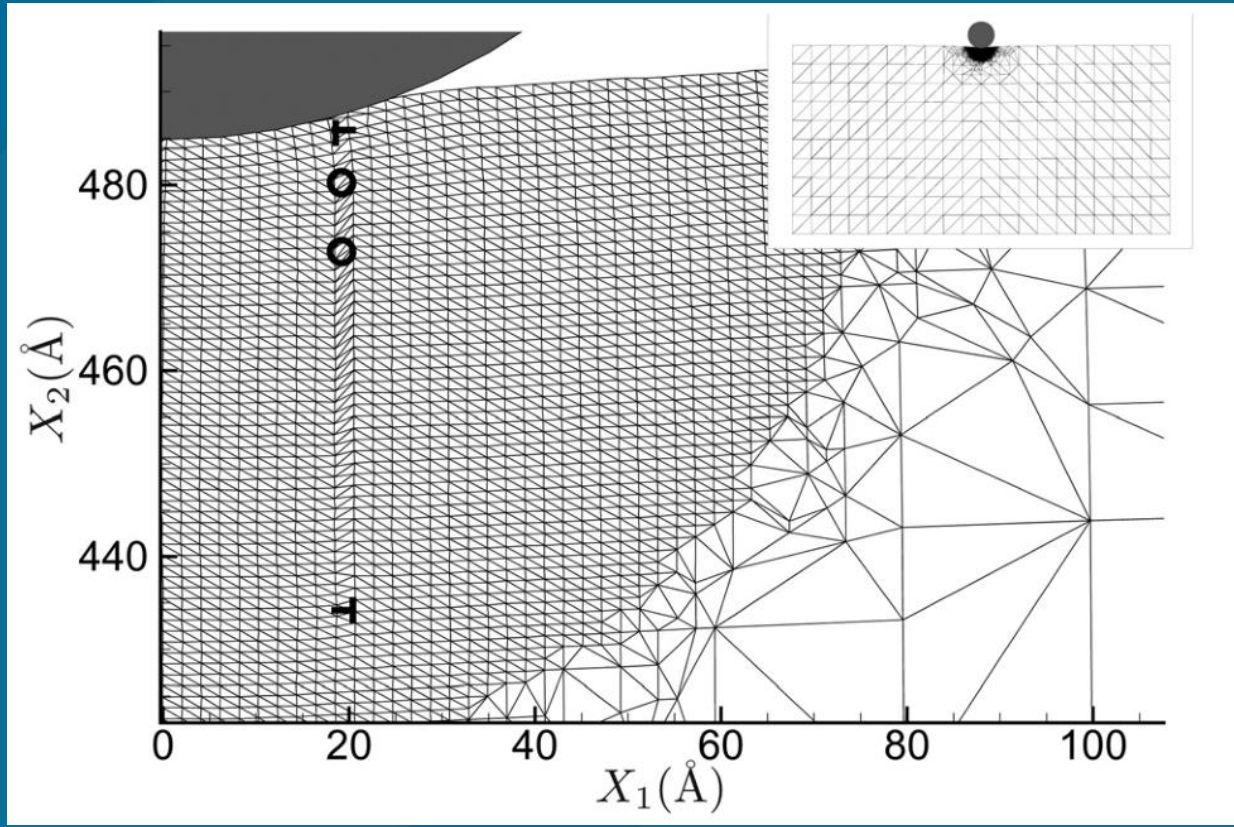

- Finite Temperature Quasicontinuum, or Hot-QC
- Requires a model for the transfer of heat between partitioned domains
- An effective Hamiltonian is derived that adequately approximates the contributions of the unrepresented atoms in the continuum region

 W.K. Kim, M. Luskin, D. Perez, A.F. Voter, E.B. Tadmor, *Journal of the Mechanics and Physics of Solids*, 2014

Hyperdynamics – Bridging Time scale

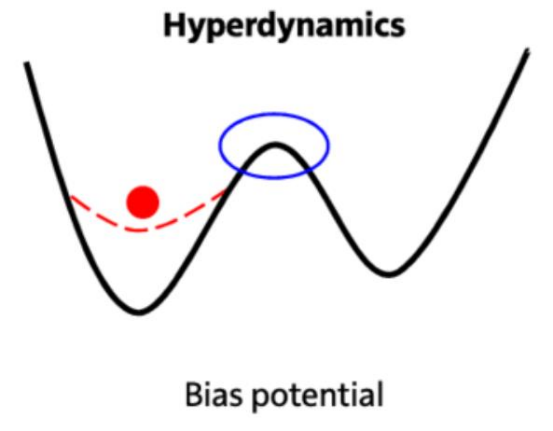

$$\Delta t_{b_i} = \Delta t_{\mathrm{MD}} e^{\beta \Delta V_b(x(t_i))}; \qquad t_b = \sum_i^{n_{\mathrm{tot}}} \Delta t_{b_i}$$

- A Bias potentials raises the energy of the system in areas other than the transition states
- Infrequent events rates boosted proportionally to the magnitude of the bias potential
- Requires no prior knowledge of the transitioning states of the system

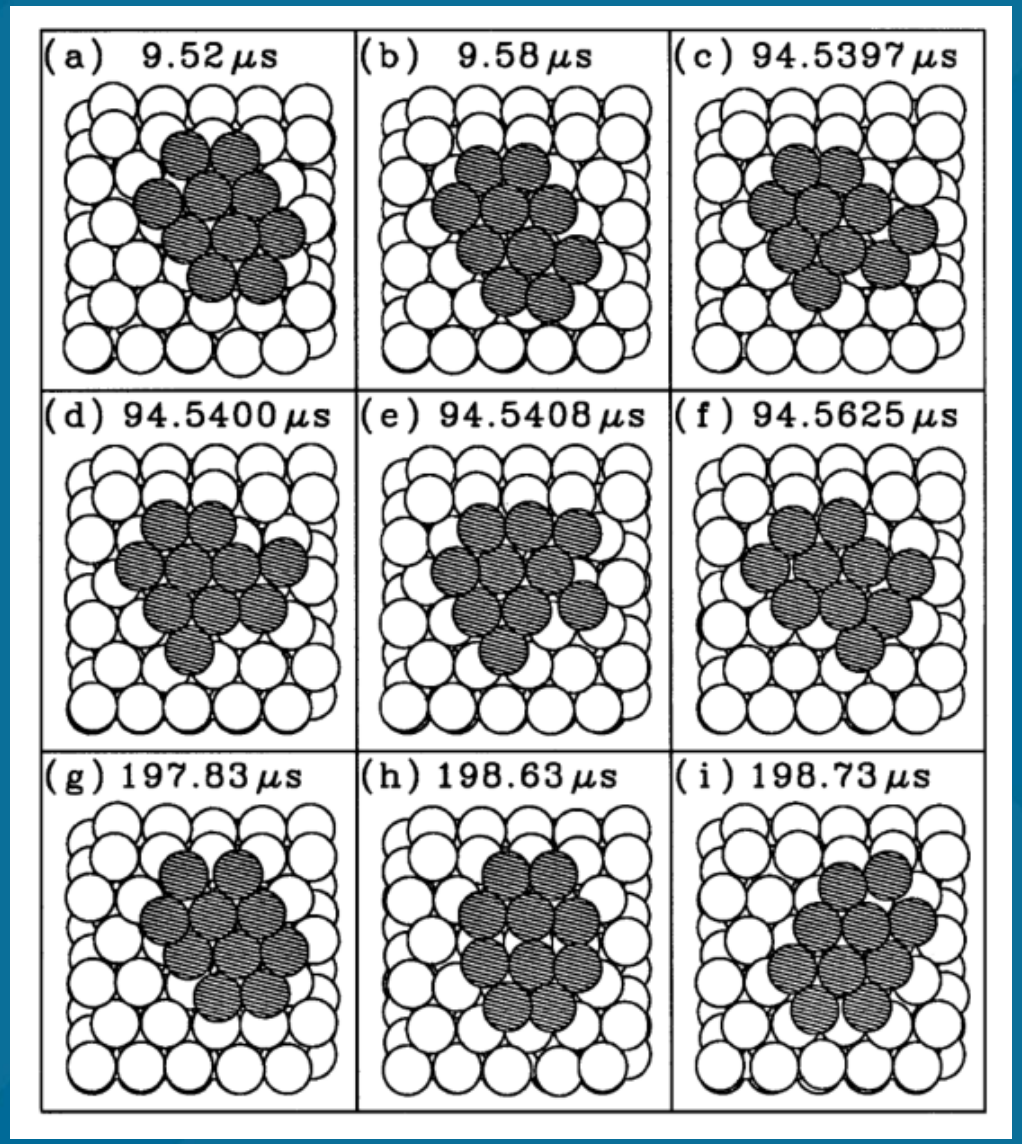

 Voter, Arthur, *Physical Review Letters*, 1997

HyperQC – Combining Spatial and Temporal Scaling

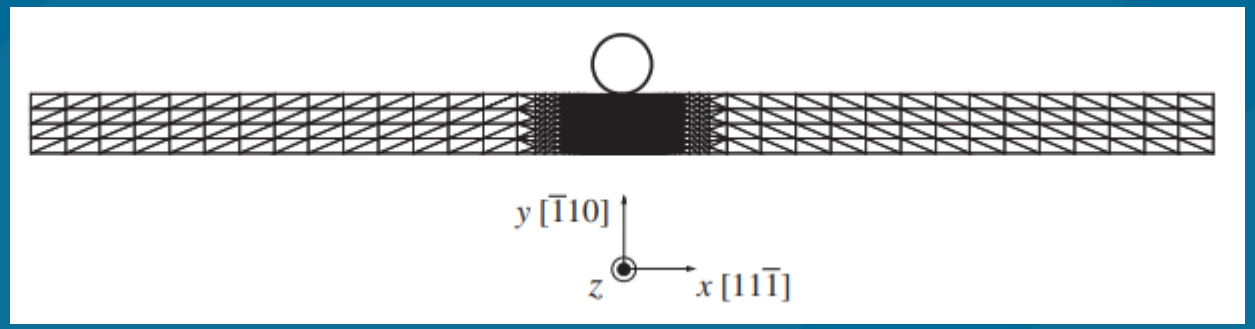

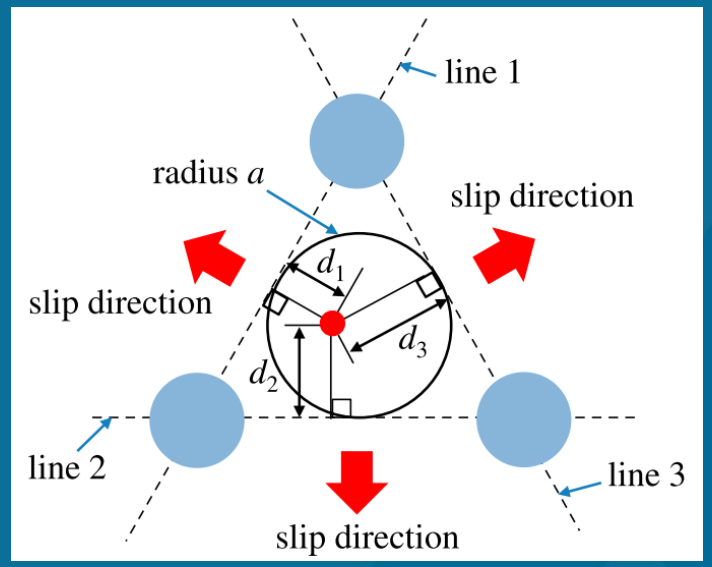

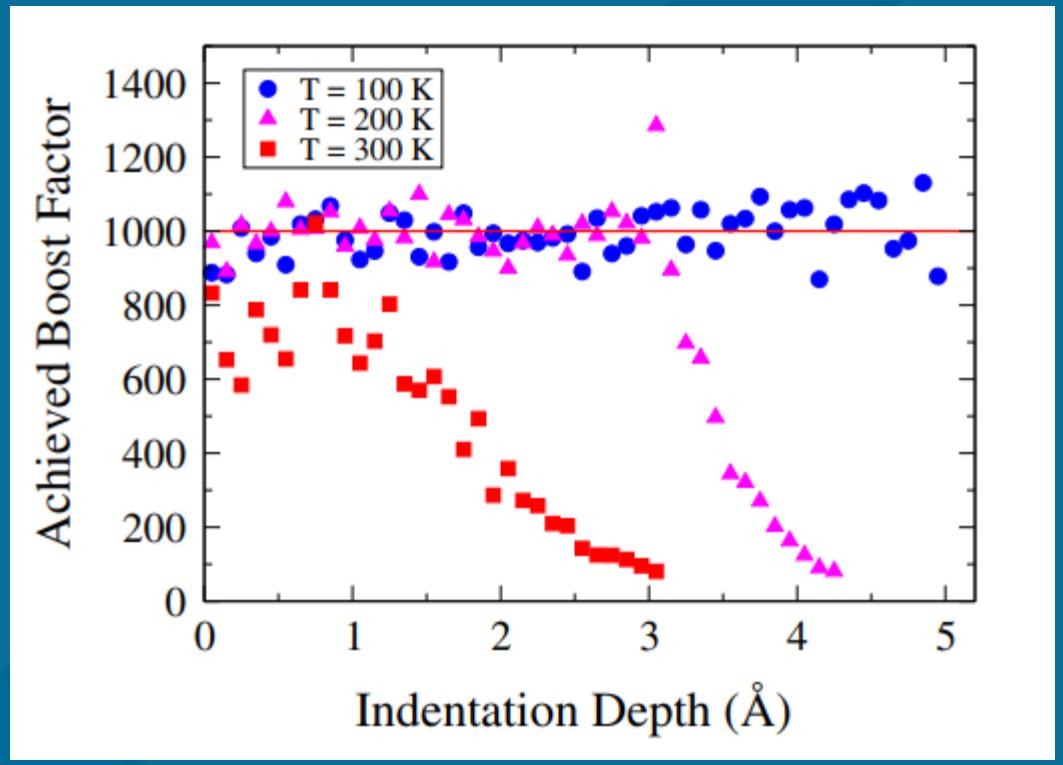

- Combining the spatial scaling of Quasicontinuum with the temporal scaling of Hyperdynamics
- A mechanism-based bias potential is applied that lowers the energy barrier for slip in fcc crystals
- Speedups between 1000 and 10000 were experienced, lowering as temperature increased

 W. K. Kim & E. B. Tadmor, *Philosophical Magazine*, 2017

Conclusion

- Empirical Potentials
  - Computationally Inexpensive
  - Based on Physical Models
  - Wide range of performance based on model used and application

- Ab Initio Calculations and Potentials
  - Based on Quantum Mechanical Methods such as Density Functional Theory
  - Extremely computationally expensive
  - Most accurate method available

- Machine Learning Potentials
  - Interpolated potentials based on data sets created from Quantum Mechanical Calculations
  - Combines the accuracy of Ab Initio with the speed of Empirical
  - Possibly the future of Molecular Dynamics Simulations

- Multiscale Methods – Quasicontinuum and Hyperdynamics
  - Bridging the gaps between length and time scales
  - Brings the possibility of simulating real-time and scale experiments

THANK YOU

UC San Diego